CPGAN: TOWARDS A BETTER GLOBAL LANDSCAPE OF GANS

Anonymous authors
Paper under double-blind review

ABSTRACT

GANs have been very popular in data generation and unsupervised learning, but our understanding of GAN training is still very limited. One major reason is that GANs are often formulated as non-convex-concave min-max optimization. As a result, most recent studies focused on the analysis in the local region around the equilibrium. In this work, we perform global analysis of GANs from two perspectives: the global landscape of the outer-optimization problem and the global behavior of the gradient descent dynamics. We find that the original GAN has exponentially many bad strict local minima which are perceived as mode-collapse, and the training dynamics (with linear discriminators) cannot escape mode collapse. To address these issues, we propose a simple modification to the original GAN, by coupling the generated samples and the true samples. We prove that the new formulation has no bad basins, and its training dynamics (with linear discriminators) has a Lyapunov function that leads to global convergence. Our experiments on standard datasets show that this simple loss outperforms the original GAN and WGAN-GP.

1 INTRODUCTION

Generative Adversarial Networks (GANs) (Goodfellow et al., 2014) have been one of the most popular methods for generating data. The original GAN minimizes the loss $\phi(p_{\mathrm{g}}, p_{\mathrm{data}}) = \max_D h_D(p_{\mathrm{g}}, p_{\mathrm{data}})$, where h_D is a binary classification loss that depends on the discriminator D. To justify the loss, Goodfellow et al. (2014) prove two theoretical results: first, for a given p_{g}, the outer function $\phi(p_{\mathrm{g}}, p_{\mathrm{data}})$ is the Jenson-Shannon (JS) distance (minus a constant); second, the outer function is convex in p_{g}, so a gradient descent method on p_{g} converges to the global minimum.

In order to further understand the training behavior of GANs, there has been a surge of interest in min-max optimization or games. One major challenge is the question about which problems to analyze. The first candidates are the two-person matrix game $\min_\psi \max_\theta \psi^T A\theta$ or general convex-concave problems. But the GAN formulation is not a convex-concave problem. As stated by Daskalakis & Panageas (2018), our knowledge of min-max optimization in non convex-concave settings is "very limited." Therefore, existing results often only analyze local stability or local convergence (Daskalakis et al., 2017; Daskalakis & Panageas, 2018; Azizian et al., 2019; Gidel et al., 2018; Mazumdar et al., 2019; Yazıcı et al., 2018; Jin et al., 2019; Sanjabi et al., 2018). Local analysis can tell us the behavior of the algorithms near the desired point, but how do we know that the algorithm will arrive there and not at some highly sub-optimal points? Answering this question requires a global landscape analysis or a study of global training dynamics.

There are some attempts on global analysis of GANs. Nagarajan & Kolter (2017) and Daskalakis et al. (2017) analyzed the simplest setting: the true data distribution is a single point and a single Gaussian distribution respectively. In these cases, the dynamics of some GANs can converge to the globally optimal solution. Thus at least in the simplest single-mode setting, there is evidence that the global landscape of (some) GANs is compelling. However, it remains unclear whether those GANs have similarly nice properties in the multi-modal setting. Again, the difficulty here is that the practical GAN formulation is not convex-concave, even for simple discriminators/generators.

Our contributions. In this work, we make a step towards understanding the global behavior of GAN training, under multi-modal settings. We focus on analyzing GANs for learning a multi-point distribution. This is a finite-sample version of the problem analyzed by Goodfellow et al. (2014), and a multi-mode extension of the Dirac-GAN problem analyzed by Nagarajan & Kolter (2017). We approach the problem from two perspectives. First, we consider the min-max optimization problem and analyze the landscape of the outer problem assuming powerful discriminators. This perspective was used by Goodfellow et al. (2014). In contrast, as optimization variables we use the samples Y instead of the probability density $p_{\rm g}$. Second, we consider the training dynamics of the game formulation assuming linear discriminators. Our contributions are summarized as follows.

- For the original GAN, we prove that the outer-minimization problem has exponentially many sub-optimal strict local minima. Each strict local minima corresponds to a mode-collapse situation.
- For both the original GAN and WGAN-GP, we prove that with linear discriminators, the training dynamics cannot escape from mode-collapse.
- We propose a new GAN formulation called CP-GAN (CoupleGAN) that enjoys nice global properties. From the first perspective, we prove that the outer-minimization problem of CP-GAN has no bad strict local minima, improving upon the original GAN. From the second perspective, we prove that with linear discriminators, the training dynamics of CP-GAN can escape from mode-collapse; in addition, it has a global Lyapunov function which permits to prove global convergence.
- Our simulation results show that the new GAN performs better than WGAN-GP and the original GAN in standard datasets. Our modification to the loss function has some similarity with the Wasserstein distance (coupling data points), but it turns out it works better than WGAN-GP on all datasets we tested. We remark that CP-GAN is orthogonal to other techniques such as spectral normalization Miyato et al. (2018), thus we only compare with vanilla methods such as WGAN-GP.

Finally, we remark that CP-GAN is just one example of GAN problems with nice global properties, and we hope our analysis can shed light on the design of other tractable GAN formulations.

Outline. The rest of the paper is structured as follows. We present the CP-GAN loss in Section 2, and discuss our analysis framework in Section 3. In Section 4, we analyze the outer-optimization problem of JS-GAN, and the training dynamics of JS-GAN and W-GAN. In Section 5, we analyze the outer-optimization problem and the training dynamics of CP-GAN. We evaluate its performance on synthetic and standard datasets in Section 6. All proofs are in Appendix.

2 Proposed Problems and New Loss

In this section, we first review the formulation of GANs briefly. Next, we present the new formulation of CP-GAN. The theoretical advantage of the new formulation will be discussed later.

2.1 Generative Adversarial Networks

We first review the formulation of the original GAN proposed by Goodfellow et al. (2014). Given samples from a true data distribution $p_{\rm data}$, we want to generate a new distribution $p_{\rm g}$ to mimic $p_{\rm data}$. To judge how far away the generated distribution $p_{\rm g}$ is from $p_{\rm data}$, a discriminator (a.k.a. critic) computes a loss value that measures their gap. This discriminator D addresses a binary classification problem, which should yield 1 for the true data point and 0 for the generated data point. The goal of the generator is to generate $p_{\rm g}$ to fool the discriminator so that the loss value is minimized. Formally, the program for a GAN is given by

$$\min_{p_{\rm g}} \max_{D} E_{x\sim p_{\rm data}, y\sim p_{\rm g}} \log(D(x)) + \log(1 - D(y)). \tag{1}$$

A common choice for the discriminator is $D(u) = \frac{1}{1+\exp(-f(u))}$, where f is a function. Given this choice, the formulation given in Eq. (1) becomes

$$\min_{p_{\rm g}} \max_{f} E_{x\sim p_{\rm data}, y\sim p_{\rm g}} \log \frac{1}{1+\exp(-f(x))} + \log \frac{1}{1+\exp(f(y))}.$$

We will use a generator $G_\theta(z)$ parameterized by θ to produce samples from a distribution p_{g}, where z is drawn from a given distribution p_z. This yields the following program:

$$\min_G \max_f E_{x\sim p_{\mathrm{data}}, z\sim p_z} \log \frac{1}{1+\exp(-f(x))} + \log \frac{1}{1+\exp(f(G(z)))}. \tag{2}$$

To resolve the vanishing gradient issue, Goodfellow et al. (2014) proposed to use a game formulation (often referred to as non-saturating GAN):

$$\max_f E_{x\sim p_{\mathrm{data}}, z\sim p_z} \log \frac{1}{1+\exp(-f(x))} + \log \frac{1}{1+\exp(f(G(z)))}, \tag{3a}$$

$$\min_G E_{x\sim p_{\mathrm{data}}, z\sim p_z} \log(1+\exp(-f(G(z)))). \tag{3b}$$

2.2 Coupling GAN

As mentioned before, the program given in Eq. (3) has shortcomings, which we propose to address via the following formulation:

$$\min_\psi \max_\theta \mathbb{E}_{x\sim p_{\mathrm{data}}, z\sim p_z} [\log \frac{1}{1+\exp(f_\theta(G_\psi(z)) - f_\theta(x))}]. \tag{4a}$$

Similar to the $-\log D$ trick used in the original GAN training (a.k.a. non-saturating GAN), in practice we always use the non-saturating version for training:

$$D \text{ problem} : \min_\theta \mathbb{E}_{x\sim p_{\mathrm{data}}, z\sim p_z}[\log(1+\exp(f_\theta(G_\psi(z)) - f_\theta(x)))], \tag{5a}$$

$$G \text{ problem} : \min_\psi \mathbb{E}_{x\sim p_{\mathrm{data}}, z\sim p_z}[\log(1+\exp(f_\theta(x) - G_\psi(z))))]. \tag{5b}$$

Here f_θ is a deep net parameterized by θ, and G_ψ is a generator net parameterized by ψ.

How would anyone discover this new loss? One simple and natural approach is based on the design of Lyapunov function: if we want to show that the sum of squares of errors is non-increasing over time, we found that a natural modification is to couple Y and X; see more details in Section 5.2.

3 Micro-GAN: Multi-Mode Generation

Mescheder (2018) quoted Rahimi: “simple experiments, simple theorems are the building blocks that help us understand more complicated systems.” Then they defined a simple model called Dirac-GAN, which uses a linear discriminator and a powerful generator to recover a single-point distribution. We define a much more general model than the Dirac-GAN. We refer to it as Micro-GAN since it resembles the microscopic analysis in statistical physics.

Definition 3.1 *The Micro-GAN consists of a generator distribution $Y = (y_1, \ldots, y_n) \in \mathbb{R}^{d\times n}$ and a discriminator $f(x)$. The true data distribution is given by a n-point distribution $X = (x_1, \ldots, x_n) \in \mathbb{R}^{d\times n}$, where x_i's are distinct.*

One motivation of the Micro-GAN is to consider an “empirical” version of the problem. Yet another motivation is construction of a simple model of multi-mode distributions: for instance, when $n = 2$, we have a two-point distribution which is the simplest two-mode distribution. We are not aware of an existing global analysis that can be applied to this simple 2-point model. As we discuss later, even for the 2-point model we can distinguish the proposed CP-GAN from existing GANs.

When analyzing an optimization formulation, it is natural to proceed in the following steps: (1) Sanity check, i.e., study whether the globally optimal solutions are desired; (2) Landscape analysis, i.e., check whether there are undesirable local minima; (3) Convergence analysis, i.e., check whether the proposed algorithm converges to a local minimum or stationary point. We will first perform a sanity check and landscape analysis (for powerful discriminators), and then study the dynamics (for linear discriminators).

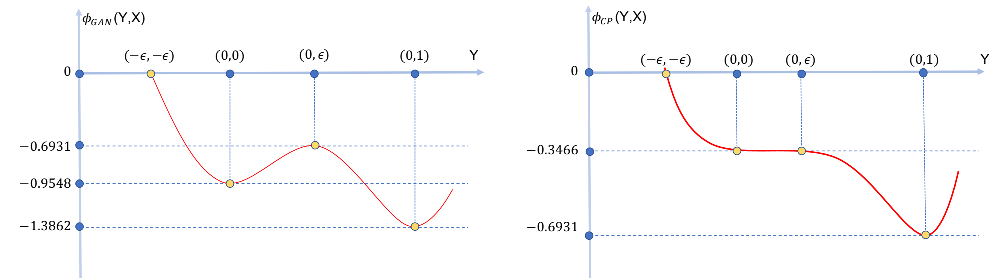

(a) original GAN (b) CP-GAN

Figure 1: Graphical illustration of the landscape of GAN outer optimization problem $\min_Y \phi(Y, X)$. It is not a rigorous figure for two reasons: (1) there are only four possible function values, thus the function is a piece-wise linear function, but we use smooth curves to connect them to make the figure easier to understand. (2) the landscape should be two-dimensional, but we only pick illustrative points and and illustrate them in 1D space.

4 Analysis of Some Existing GANs

4.1 JS-GAN has Many Bad Basins

We analyze the landscape of JS-GAN under the Micro-GAN model with powerful discriminators, the formulation of which can be written as:

$$\min_{Y \in \mathbb{R}^n} \phi_{\text{JS}}(Y, X) \triangleq \max_f L^{\text{JS}}(f; Y), \tag{6}$$

where $L^{\text{JS}}(f; Y) = -\frac{1}{n} \sum_{i=1}^n \log(1 + \exp(-f(x_i)) - \sum_{i=1}^n \log(1 + \exp(f(y_i)))$.

The range of $\phi_{\text{JS}}(Y, X)$ is $[-2 \log 2, 0]$ because $L^{\text{JS}}(f; Y) \leq 0$ and $\phi_{\text{JS}}(Y, X) \geq L(0; Y) = -2 \log 2$, where $L(0; Y)$ represents the value achieved at $f = 0$.

To build intuition, we first present a result for the case of $n = 2$ points.

Claim 4.1 *Suppose $n = 2$ and $x_1 \neq x_2 \in \mathbb{R}^d$. Then*

$$\phi_{\text{JS}}(Y, X) = \begin{cases} -2 \log 2 \approx -1.3862, & \text{if } \{x_1, x_2\} = \{y_1, y_2\} \\ -\log 2 \approx -0.6931, & \text{if } |\{x_1, x_2\} \cap \{y_1, y_2\}| = 1, \\ \log 2 - 1.5 \log 3 \approx -0.9548, & \text{if } y_1 = y_2 \in \{x_1, x_2\}, \\ 0 & \text{if } |\{x_1, x_2\} \cap \{y_1, y_2\}| = \emptyset. \end{cases}$$

The global minimum is $-2 \log 2$, which is achieved iff the generated data points $\{y_1, y_2\}$ coincide with the true data points $\{x_1, x_2\}$.

As a corollary of the above claim, the outer optimization objective of the original GAN has a bad strict local-min when two points overlap (a mode-collapse).

Corollary 4.1 *Suppose $n = 2$ and $x_1 \neq x_2 \in \mathbb{R}^d$. Then $\bar{Y} = (x_1, x_1)$ is a sub-optimal strict local minimum of the function $g(Y) = \phi_{\text{JS}}(Y, X)$.*

We illustrate the landscape of $\phi_{\text{JS}}(Y, X)$ in Figure 1a for the special case that $d = 1, x_1 = 0, x_2 = 1$. In this case, $Y = (y_1, y_2) = (0, 1)$ is the global minimum of $\phi_{\text{JS}}(Y, X)$ with optimal value $-2 \log 2 \approx -1.3862$, and $Y = (0, 0)$ is a strict local minimum of $\phi_{\text{JS}}(Y, X)$ with value approximately -0.9548. An intuitive way to understand the landscape and Corollary 4.1 is given as follows. Consider a point (y_1, y_2) moving from $(0, 1)$ to $(-0.1, -0.1)$, going through four points: $(y_1, y_2) = (0, 1)$, $(0, 0.5)$, $(0, 0)$, and finally $(-0.1, -0.1)$. The four points correspond to the four cases above, thus giving values $-1.3862, -0.6931, -0.9548, 0$. The four values are not monotone, indicating that there is a strict local minimum at -0.9538.

For general n, the landscape can be characterized in a similar fashion. The following result states that the original GAN objective has exponentially many strict bad local minima.

Proposition 1 *Suppose $x_1, x_2, \ldots, x_n \in \mathbb{R}^d$ are distinct. Consider the problem in Eq.* (6)*.*

(i) The global minimal value is $-2\log 2$, which is achieved iff the generated data points coincide with the true data points, i.e., $\{y_1, \ldots, y_n\} = \{x_1, \ldots, x_n\}$.

(ii) If $y_i \in \{x_1, \ldots, x_n\}, i = 1, 2, \ldots, n$ and $y_i = y_j$ for some $i \neq j$, then Y is a sub-optimal strict local minimum. Therefore, $\phi_{\mathrm{JS}}(\cdot, X)$ has $(n^n - n!)$ sub-optimal strict local minima.

The landscape analysis is a high-level analysis that provides some preliminary insight into the training process. But there are two gaps compared to the true training process: (1) in practice, we always use different objectives for D and G (the $-\log D$ trick) to resolve the gradient vanishing issue; (2) the D problem is addressed via a few gradient steps only. We suspect that the major insight conveyed in the landscape analysis can still carry over to the training dynamics for the following reasons: (1) the objectives for D and G are still closely related thus the "landscape" is still similar (this can be proved rigorously by considering a bi-level optimization problem, which we skip here); (2) inexactly optimizing D can smooth the landscape, so that the flat regions in $\phi^{\mathrm{JS}}(\cdot, X)$ becomes smooth (this may be why having a discontinuous outer-function is not too big an issue of JS-GAN). However, we suspect that this smoothing effect cannot easily eliminate some deep basins, especially when there are exponentially many. A complete analysis of this effect is beyond the scope of this paper, and we will just show some evidence by analyzing the training dynamics of JS-GAN with linear discriminators.

4.2 Training Dynamics of JS-GAN

We consider the non-saturating version of the formulation in Eq. (6), which is also the finite-sample version of Eq. (3). We assume a linear discriminator $f(u) = w^T u + b$, where $w \in \mathbb{R}^d$, $b \in \mathbb{R}$.

$$\min_{\theta=(w,b)\in\mathbb{R}^d\times\mathbb{R}} L^D_{\mathrm{GAN}}(Y;\theta) \triangleq \sum_{i=1}^n \log(1+\exp(-w^T x_i - b)) + \log(1+\exp(w^T y_i + b)),$$

$$\min_{Y=(y_1,\ldots,y_n)\in\mathbb{R}^{d\times n}} L^G_{\mathrm{GAN}}(Y;\theta) \triangleq \sum_{i=1}^n \log(1+\exp(-w^T y_i - b)).$$

Consider the dynamics corresponding to the simultaneous gradient descent (GD) [1]:

$$\frac{dw}{dt} = -\frac{\partial L^D_{\mathrm{GAN}}}{\partial w} = \sum_{i=1}^n \frac{x_i}{1+e^{w^T x_i + b}} - \frac{y_i}{1+e^{-w^T y_i - b}}, \tag{7a}$$

$$\frac{db}{dt} = -\frac{\partial L^D_{\mathrm{GAN}}}{\partial b} = \sum_{i=1}^n \frac{1}{1+e^{w^T x_i + b}} - \frac{1}{1+e^{-w^T y_i - b}}, \tag{7b}$$

$$\frac{dy_i}{dt} = -\frac{\partial L^G_{\mathrm{GAN}}}{\partial y_i} = \frac{w}{1+e^{w^T y_i + b}}. \tag{7c}$$

The common method to deal with such complicated dynamics is local linearization. This permits to analyze the local behavior of the dynamics (see, e.g., Mescheder et al. (2018)). A global analysis of the dynamics often requires a proper Lyapunov function that is non-increasing along the trajectories. But the design of Lyapunov functions is often challenging.

Even if one does not find such a function, one may wonder whether this is due to the lack of technical tools, or due to some intrinsic barriers. Motivated by the landscape result in Proposition 1, we wish to analyze the mode-collapse patterns, i.e., the pattern occurring when some points overlap. Interestingly, we find that collapsed modes cannot be recovered under JS-GAN dynamics, as formally stated in the following claim:

Claim 4.2 *Starting from any initial point $(\theta(0), Y(0))$, the trajectory $(\theta(t), Y(t))$ defined in Eq.* (13) *satisfies $\|y_i(t) - y_j(t)\| \leq \|y_i(0) - y_j(0)\|, \forall t$.*

[1] Other papers, such as Mescheder (2018) analyzed both simultaneous GD and alternating GD. For simplicity, we only analyze simultaneous GD in this paper.

This claim predicts that starting from $y_1(0) = y_2(0) = \cdots = y_n(0)$ (all points fall into one mode), prevents these points from separating. It is interesting to more rigorously characterize bad global behavior of JS-GAN dynamics, either for a linear or a neural-net discriminator (e.g., whether mode-collapse patterns create bad attractors or limit cycles). Anyhow, the above claim makes it very hard, if not impossible, to prove the global convergence of JS-GAN dynamics for multi-mode problems.

4.3 Discussions of WGAN and its variants

One may wonder whether W-GAN or its variants can provide a solution to the above issues. We briefly discuss the difficulties in a global analysis of WGAN and its variants.

For W-GAN with Lipschitz constrain on f, it is not hard to prove that the outer-optimization problem has a nice landscape. However, it is hard to impose the Lipschitz condition in practice; in addition, gradient dynamics with constraints are difficult to analyze [2].

A practical solution to resolve the Lipschitz constraint issue is to add a gradient penalty, which recovers WGAN-GP Gulrajani et al. (2017). However, the outer-optimization problem $\min_Y \max_f \sum_i f(x_i) - \sum_i f(y_i) - \lambda \sum_i (\|\nabla_u f(u) \mid_{u=y_i} \| - 1)^2$ may have a complicated landscape due to the extra regularization term.

We further show that the dynamics of WGAN-GP with linear discriminators has a similar issue to JS-GAN. The details are provided in Appendix.

Claim 4.3 *Starting from any initial point* $(w(0), Y(0))$*, the trajectory* $(w(t), Y(t))$ *defined by WGAN-GP dynamics satisfies* $\|y_i(t) - y_j(t)\| = \|y_i(0) - y_j(0)\|, \forall t$.

To avoid additional issues due to constraints, we remain interested in the logistic function used in the JS-GAN formulation. We hope that a small modification to the JS-GAN directly addresses its issues. We will now show that CP-GAN does achieve this goal.

5 Analysis of CP-GAN

In this section, we analyze the proposed new CP-GAN formulation, and show that it has an advantage over the original GAN framework. We highlight again a major difference of our analysis compared to earlier works: we focus on global analysis while most existing results focus on local analysis.

5.1 CP-GAN has No Bad Basin

Following the aforementioned steps, the finite-sample version of CP-GAN reads

$$\min_Y \phi_{\mathrm{CP}}(Y, X), \text{ where } \phi_{\mathrm{CP}}(Y, X) \triangleq \sup_f \frac{1}{n} \sum_{i=1}^{n} \log \frac{1}{1 + \exp(f(y_i) - f(x_i)))}, \tag{8}$$

resulting in a range $\phi_{\mathrm{CP}}(Y, X) \in [-\log 2, 0]$. For simplicity, we define $g^{\mathrm{CP}}(Y) = \phi_{\mathrm{CP}}(Y, X)$ as the data X are fixed throughout the paper.

Proposition 2 *Suppose* $x_1, x_2, \ldots, x_n \in \mathbb{R}^d$ *are distinct. The global minimal value of* $g^{\mathrm{CP}}(Y)$ *is* $-\log 2$*, which is achieved iff* $\{x_1, \ldots, x_n\} = \{y_1, \ldots, y_n\}$*. Furthermore, for any* Y*, there is a continuous path from* Y *to a global minimum along which the value of* $g^{\mathrm{CP}}(Y)$ *is non-increasing.*

To understand this result, consider the special case $n = 2$ and $x_1 \neq x_2 \in \mathbb{R}^d$. In this case, we have

$$\phi_{\mathrm{CP}}(Y, X) = \begin{cases} -\log 2 \approx -0.6931, & \text{if } \{x_1, x_2\} = \{y_1, y_2\} \\ -\frac{1}{2}\log 2 \approx -0.3466, & \text{if } |\{i : x_i = y_i\}| = 1 \\ 0 & \text{otherwise.} \end{cases}$$

[2]Mescheder (2018) analyzed W-GAN dynamics, but only consider the local region around 0, thus its analysis essentially ignores the Lipschitz constraint.

We illustrate the landscape of $g^{\mathrm{CP}}(Y)$ in Figure 1b for the special case that $n = 2, d = 1, x_1 = 0, x_2 = 1$. In this case, $(y_1, y_2) = (0, 1)$ and $(y_1, y_2) = (1, 0)$ are two global minima of $g^{\mathrm{CP}}(Y)$ with optimal value $-\log 2 \approx -0.6931$. Similar to the previous subsection, there is an intuitive way to understand the landscape: Consider a point (y_1, y_2) moving from $(0, 1)$ to $(-0.1, -0.1)$, going through four points: $(y_1, y_2) = (0, 1)$, then $(0, 0.5)$, then $(0, 0)$, and finally $(-0.1, -0.1)$. The four points correspond to four values $-0.6931, -0.3466, -0.3466, 0$. The four values are non-decreasing, indicating that there is a monotone path connecting the mode-collapsed pattern $(0, 0)$ and a global-min $(0, 1)$. This is different from the landscape of the JS-GAN loss, where any path between the two points has to cross some barrier.

Comparing Proposition 2 and Proposition 1, we observe the landscape of CP-GAN to be better than that of the original GAN formulation. How does that help training? Intuitively, the original GAN landscape has many basins of attraction. When starting a random initial point, a descent algorithm might fall into one of the bad basins, causing mode collapse. For CP-GAN, the only basin of attraction is the global minimum, thus the algorithm is more likely to converge to the global minimum.

5.2 Training Dynamics of CP-GAN

Next, we consider the training dynamics of CP-GAN, and reveal nice global properties. Consider the game variant of the GAN formulation in Eq. (8), i.e., the finite-sample version of Eq. (5). Further, we assume the linear discriminator $f(u) = w^T u$, where $w \in \mathbb{R}^d$:

$$\min_{\theta = w \in \mathbb{R}^d} L_{\mathrm{CP}}^D(Y; \theta) \triangleq \sum_{i=1}^n \log(1 + \exp(w^T(y_i - x_i))),$$
$$\min_{Y = (y_1, \ldots, y_n) \in \mathbb{R}^{d \times n}} L_{\mathrm{CP}}^G(Y; \theta) \triangleq \sum_{i=1}^n \log(1 + \exp(w^T(x_i - y_i))).$$

Consider the dynamics corresponding to the simultaneous gradient descent for CP-GAN:

$$\frac{dw}{dt} = -\frac{\partial L_{\mathrm{CP}}^D}{\partial w} = \sum_{i=1}^n \frac{x_i - y_i}{1 + e^{w^T(x_i - y_i)}}, \tag{9a}$$
$$\frac{dy_i}{dt} = -\frac{\partial L_{\mathrm{CP}}^G}{\partial y_i} = \frac{w}{1 + e^{w^T(y_i - x_i)}}. \tag{9b}$$

Define $\delta_i = y_i - x_i, \forall i$. Define function $\beta_{ij}(t) = \frac{1}{2}\|\delta_i(t) - \delta_j(t)\|^2, \forall\, i, j$.

Claim 5.1 *Along the trajectory defined by Eq.* (9)*, we have* $\|(\delta_i(t) - \delta_j(t)\| \le \|(\delta_i(0) - \delta_j(0)\|, \forall i, j$.

This claim looks similar to the result for the JS-GAN dynamics given in Claim 4.2. However, there is an important difference. For the original GAN, the gaps between *generated samples* are shrinking, while for CP-GAN, the gaps between the *errors* are shrinking. Thus CP-GAN is a more natural choice from this perspective.

This claim only shows the difference of the two GAN formulations, and we will show that CP-GAN has the extra benefit that it has a natural potential function. Consider the function

$$V = \frac{1}{2}\|w\|^2 + \frac{1}{2}\sum_{i=1}^n \|x_i - y_i\|^2.$$

Obviously, $V = 0$ iff $w = 0$ and $x_i = y_i, \forall i$. According to the following result, V is non-increasing along the trajectory of CP-GAN training.

Claim 5.2 *Along the trajectory of the dynamics defined in Eq.* (9)*, we have* $\frac{dV(t)}{dt} \le 0$.

Thus V is a Lyapunov function for the CP-GAN dynamics. As mentioned earlier Mescheder (2018) showed that V is a Lyapunov function for the JS-GAN dynamics (non-saturating version) given in Eq. (13) if $n = 1$ and $x_1 = 0$. However, when we check the case $x_1 \neq 0$, we found it is no

Model	MNIST		CIFAR10		CelebA		LSUN	
	IS	FID	IS	FID	IS	FID	IS	FID
NSGAN	1.87±0.03	24.01	4.73±0.24	53.01	2.84±0.08	20.52	2.87±0.08	28.28
WGAN-GP	1.94±0.03	17.53	5.14±0.15	44.11	2.89±0.11	17.18	3.19±0.10	24.26
CPGAN	1.99±0.02	12.39	5.33±0.20	37.57	2.95±0.07	16.02	3.39±0.04	22.94

Table 1: Inception score (IS) (higher is better) and Frechét Inception distance (FID) (lower is better) for non-saturating GAN, WGAN-GP and our proposed CPGAN on MNIST, CIFAR10, CelebA and LSUN.

longer a Lyapunov function. This means that the JS-GAN formulation is not "translation invariant" in the sense that shifting x_i and y_i together leads to different dynamics. A simple fix to make it shift-invariant is to couple Y and X together.

With the Lyapunov function, we have the global convergence to the set θ such that $\langle \nabla_\theta V(\theta), h(\theta)\rangle = 0$, where h is the right-hand side of Eq. (9). With a bit more effort, we can show the convergence of CP-GAN dynamics to the set of stationary points for $d = 1$.

Proposition 3 *(global convergence of CP-GAN dynamics) When $d = 1$, starting from any initial point $\theta(0)$, the trajectory defined by the CP-GAN dynamics $\theta(t)$ will satisfy $\lim_{t\to\infty} \theta(t) \in M$, where $M = \{(w, y) : w = 0, \sum_i x_i = \sum_i y_i\}$.*

The set of stationary points include some undesired points. The next result shows that the Jacobian at these undesired points have positive real part, thus they are not stable. Simulations also show that small perturbation can escape these undesired points.

Claim 5.3 *When $d = 1$, for the training dynamics given in Eq. (9), at any point other than the desired solution $(y_1, \ldots, y_n) = (x_1, \ldots, x_n)$ in the set of stationary solutions, the Jacobian has an eigenvalue with positive real part.*

Now we have a clear understanding of the global behavior of the training dynamics of CP-GAN. The most important fact is that the energy function V is a Lyapunov function. There may be other loss functions that have a Lyapunov function, at least in the simple setting, and we leave that exploration to future work.

6 Experiments

In this section, we present empirical results comparing different GAN loss functions. We aim to show the qualitative and quantitative improvements achieved by using the proposed loss.

6.1 Synthetic Datasets

We first demonstrate our results on 2-dimensional synthetic data. Specifically, the 2-dimensional data $x = (x_1, x_2)$ is drawn from a mixture of 5 or 25 equally weighted Gaussians each with a variance of 0.002, the means of which are spaced equally on the unit circle. See the blue points in columns (a) and (d) of figure 2 for an illustration. Our generated samples are shown as the red points in (a) and (c) in figure 2 and we can see our generators can catch every mode. The generator and the discriminator loss are shown in (b), (c), (e) and (f).

6.2 Image Generation

In this section, we present results on the task of image generation. We train and evaluate CPGAN on four datasets: (1) MNIST (LeCun et al., 1998) (32×32); (2) CIFAR-10 (Krizhevsky, 2009) (32×32); (3) CelebA (Liu et al., 2015) (64×64); and (4) LSUN Bedrooms (Yu et al., 2015) (64×64). We use the Spectral Normalization GAN structure for MNIST, and the DCGAN structure for CIFAR-10, CelebA and LSUN. The input size for the generator is 128-dimensional.

(a) (b) (c) (d) (e) (f)

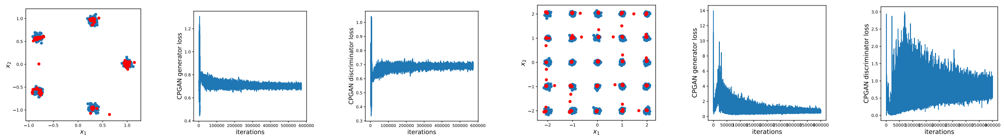

Figure 2: (a) True(blue) and generated(red) Samples (b) loss for the generator (c) loss for the discriminator from 5-Gaussian synthetic data. (d) True(blue) and generated(red) Samples (e) loss for the generator (f) loss for the discriminator from 25-Gaussian synthetic data.

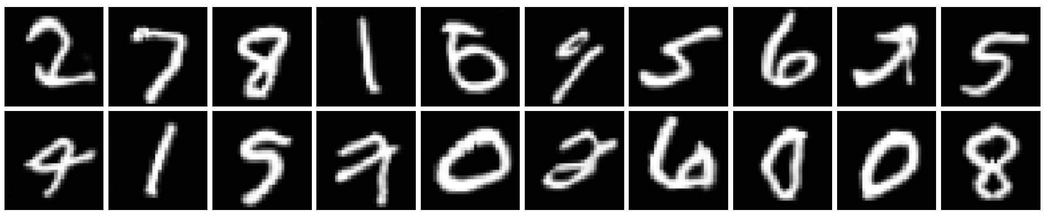

(a)

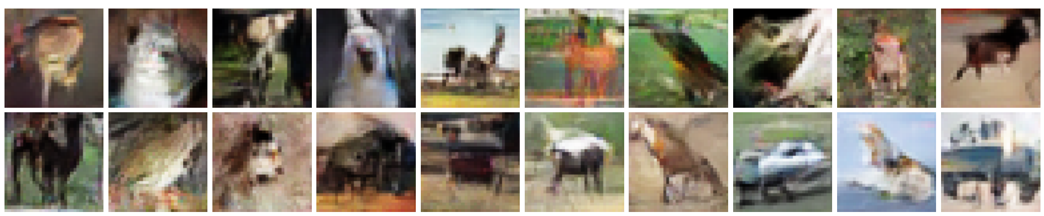

(b)

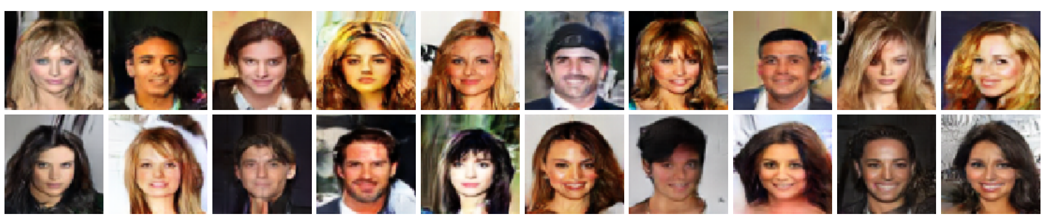

(c)

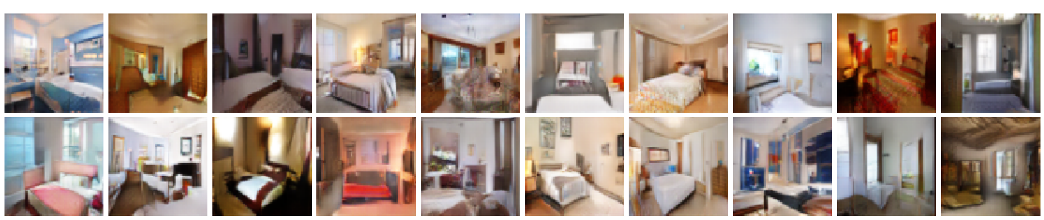

(d)

Figure 3: Generated (a)MNIST (b) CIFAR-10 (c) CelebA (d) LSUN samples by CPGAN.

In all our experiments we train the generator and discriminator in an alternating fashion. The batch size is set to 100. We trained the generator and the discriminator each for $30k$ batch iterations on the MNIST dataset, and for $100k$ iterations on the CIFAR-10, CelebA and LSUN datasets. We tuned the learning rate for each model to achieve their best performance. Some generated samples are shown in figure 3.

We use inception scores (IS) (Salimans et al., 2016) and Frechét Inception distance (FID) (Heusel et al., 2017) to assess the quality of the generated images. We used $5k$ true images and $5k$ generated images for IS and FID metric calculation respectively. We provide the results in Table 1. We observe the proposed loss to perform better than other losses in terms of FID scores, on all data sets.

REFERENCES

Waïss Azizian, Ioannis Mitliagkas, Simon Lacoste-Julien, and Gauthier Gidel. A tight and unified analysis of extragradient for a whole spectrum of differentiable games. *arXiv preprint arXiv:1906.05945*, 2019.

Cyril Cohen and Damien Rouhling. A formal proof in coq of lasalles invariance principle. In *International Conference on Interactive Theorem Proving*, pp. 148–163. Springer, 2017.

Constantinos Daskalakis and Ioannis Panageas. The limit points of (optimistic) gradient descent in min-max optimization. In *Advances in Neural Information Processing Systems*, pp. 9236–9246, 2018.

Constantinos Daskalakis, Andrew Ilyas, Vasilis Syrgkanis, and Haoyang Zeng. Training gans with optimism. *arXiv preprint arXiv:1711.00141*, 2017.

Gauthier Gidel, Reyhane Askari Hemmat, Mohammad Pezeshki, Remi Lepriol, Gabriel Huang, Simon Lacoste-Julien, and Ioannis Mitliagkas. Negative momentum for improved game dynamics. *arXiv preprint arXiv:1807.04740*, 2018.

Ian Goodfellow, Jean Pouget-Abadie, Mehdi Mirza, Bing Xu, David Warde-Farley, Sherjil Ozair, Aaron Courville, and Yoshua Bengio. Generative adversarial nets. In *Advances in neural information processing systems*, pp. 2672–2680, 2014.

Ishaan Gulrajani, Faruk Ahmed, Martin Arjovsky, Vincent Dumoulin, and Aaron Courville. Improved training of wasserstein gans. *arXiv preprint arXiv:1704.00028*, 2017.

Wassim M Haddad and VijaySekhar Chellaboina. *Nonlinear dynamical systems and control: a Lyapunov-based approach*. Princeton university press, 2011.

Martin Heusel, Hubert Ramsauer, Thomas Unterthiner, Bernhard Nessler, and Sepp Hochreiter. Gans trained by a two time-scale update rule converge to a local nash equilibrium. In *Advances in Neural Information Processing Systems*, pp. 6629–6640, 2017.

Chi Jin, Praneeth Netrapalli, and Michael I Jordan. Minmax optimization: Stable limit points of gradient descent ascent are locally optimal. *arXiv preprint arXiv:1902.00618*, 2019.

Alex Krizhevsky. Learning multiple layers of features from tiny images. 2009.

Yann LeCun, Corinna Cortes, and Christopher JC Burges. The mnist database of handwritten digits, 1998.

Ziwei Liu, Ping Luo, Xiaogang Wang, and Xiaoou Tang. Deep learning face attributes in the wild. In *Proceedings of International Conference on Computer Vision (ICCV)*, 2015.

Eric V Mazumdar, Michael I Jordan, and S Shankar Sastry. On finding local nash equilibria (and only local nash equilibria) in zero-sum games. *arXiv preprint arXiv:1901.00838*, 2019.

Lars Mescheder. On the convergence properties of gan training. *arXiv preprint arXiv:1801.04406*, 1:16, 2018.

Lars Mescheder, Andreas Geiger, and Sebastian Nowozin. Which training methods for gans do actually converge? *arXiv preprint arXiv:1801.04406*, 2018.

Takeru Miyato, Toshiki Kataoka, Masanori Koyama, and Yuichi Yoshida. Spectral normalization for generative adversarial networks. *arXiv preprint arXiv:1802.05957*, 2018.

Vaishnavh Nagarajan and J Zico Kolter. Gradient descent gan optimization is locally stable. In *Advances in Neural Information Processing Systems*, pp. 5585–5595, 2017.

Tim Salimans, Ian Goodfellow, Wojciech Zaremba, Vicki Cheung, Alec Radford, Xi Chen, and Xi Chen. Improved techniques for training gans. In D. D. Lee, M. Sugiyama, U. V. Luxburg, I. Guyon, and R. Garnett (eds.), *Advances in Neural Information Processing Systems 29*, pp. 2234–2242. Curran Associates, Inc., 2016. URL `http://papers.nips.cc/paper/6125-improved-techniques-for-training-gans.pdf`.

Maziar Sanjabi, Jimmy Ba, Meisam Razaviyayn, and Jason D Lee. On the convergence and robustness of training gans with regularized optimal transport. In *Advances in Neural Information Processing Systems*, pp. 7091–7101, 2018.

Yasin Yazıcı, Chuan-Sheng Foo, Stefan Winkler, Kim-Hui Yap, Georgios Piliouras, and Vijay Chandrasekhar. The unusual effectiveness of averaging in gan training. *arXiv preprint arXiv:1806.04498*, 2018.

Fisher Yu, Ari Seff, Yinda Zhang, Shuran Song, Thomas Funkhouser, and Jianxiong Xiao. Lsun: Construction of a large-scale image dataset using deep learning with humans in the loop. *arXiv preprint arXiv:1506.03365*, 2015.

A Proofs in Section 4.1

A.1 Proof of Claim 4.1

We will compute values of $\phi_{\text{JS}}(Y, X)$ for all Y.

Denote $D(u) = \frac{1}{1+\exp(-f(u))} \in [0, 1]$. Since f can be any continuous function, D can be any continuous function with range $(0, 1)$.

$$\begin{aligned}\phi_{\text{JS}}(Y, X) &= \sup_f \frac{1}{n} \sum_{i=1}^n \log \frac{1}{1+\exp(-f(x_i))} + \sum_{i=1}^n \log \frac{1}{1+\exp(f(y_i))} \\ &= \sup_D \frac{1}{n} \sum_{i=1}^n \log(D(x_i)) + \sum_{i=1}^n \log(1 - D(y_i)).\end{aligned}$$

Consider four cases.

Case 1: Both generated points overlap with the true data points, and are distinct, i.e., $y_1 = x_1, y_2 = x_2$ or $y_2 = x_1, y_2 = x_2$. Then the objective is

$$\sup_D \frac{1}{2} \log(D(x_1)) + \frac{1}{2} \log(1 - D(x_1)) + \frac{1}{2} \log(D(x_2)) + \frac{1}{2} \log(1 - D(x_2))$$

The optimal value is $-2 \log 2$, which is achieved when $D(x_1) = D(x_2) = 1$. The corresponding function values of f are $f(x_1) = f(x_2) = 0$. The values of f on other points do not matter.

Case 2: Exactly one of the generated points overlaps with the true data points. Without loss of generality, we can check the case $y_1 = x_1, y_2 \notin \{x_1, x_2\}$. The problem becomes

$$\sup_D \frac{1}{2} \log(D(x_1)) + \frac{1}{2} \log(D(x_2)) + \frac{1}{2} \log(1 - D(x_1)) + \frac{1}{2} \log(1 - D(y_2)).$$

The optimal value $-\log 2 \approx -0.6931$ is achieved when $D(x_1) = 1/2$, $D(x_2) = 1$ and $D(y_2) = 0$.

Case 3: Both generated points overlap with the true data points, and are the same. Without loss of generality, check the case $y_1 = y_2 = x_1$.

$$\sup_D \frac{1}{2} \log(D(x_1)) + \log(1 - D(x_1)) + \frac{1}{2} \log(D(x_2)).$$

The optimal value $\frac{1}{2} \log \frac{1}{3} + \log \frac{2}{3} \approx -0.9548$ is achieved when $D(x_1) = 1/3$ and $D(x_2) = 0$.

Case 4: Both generated points are different from the true data points. $y_1, y_2 \notin \{x_1, x_2\}$. It becomes separable over the four points

$$\sup_D \frac{1}{2} \log(D(x_1)) + \frac{1}{2} \log(D(x_2)) + \frac{1}{2} \log(1 - D(y_1)) + \frac{1}{2} \log(1 - D(y_2)).$$

Each term can achieve its maximum $\log 1 = 0$. Thus the optimal value 0 is achieved when $D(x_1) = D(x_2) = 1$ and $D(y_1) = D(y_2) = 0$.

A.2 PROOF OF COROLLARY 4.1

We re-state the corollary below.

Corollary A.1 *Suppose $\bar{Y} = (\bar{y}_1, \bar{y}_2)$ satisfies $\bar{y}_1 = \bar{y}_2 = x_1$, then it is a sub-optimal strict local minimum of the problem.*

Proof: Suppose ϵ is the minimal non-zero distance between two points of x_1, x_2, y_1, y_2. Consider a small perturbation of $\bar{Y}$ as $Y = (\bar{y_1} + \epsilon_1, \bar{y_2} + \epsilon_2)$, where $|\epsilon_i| < \epsilon$. We want to verify that

$$\phi(\bar{Y}, X) > \phi(Y, X) \approx -0.9548. \tag{10}$$

There are two possibilities.

Possibility 1: $\epsilon_1 = 0$ or $\epsilon_2 = 0$. WLOG, assume $\epsilon_1 = 0$, then we must have $\epsilon_2 > 0$. Then we still have $y_1 = \bar{y}_1 = x_1$. Since the perturbation amount is small enough, we have $y_2 \notin \{x_1, x_2\}$. According to Case 2 above, we have

$$\phi(\bar{Y}, X) = -\log 2 \approx -0.6931 > -0.9548.$$

Possibility 2: $\epsilon_1 > 0, \epsilon_2 > 0$. Since the perturbation amount ϵ_1 and ϵ_2 are small enough, we have $y_1 \notin \{x_1, x_2\}, y_2 \notin \{x_1, x_2\}$. According to Case 4 above, we have

$$\phi(\bar{Y}, X) = 0 > -0.9548.$$

Combining both cases, we have proved (11).

Q.E.D.

A.3 PROOF OF PROPOSITION 1

Denote $D(u) = \frac{1}{1+\exp(-f(u))} \in [0, 1]$. Since f can be any continuous function, D can be any continuous function with range $(0, 1)$.

$$\begin{aligned}
\phi_{\mathrm{JS}}(Y, X) &= \sup_f \frac{1}{n} \sum_{i=1}^n \log \frac{1}{1 + \exp(-f(x_i))} + \sum_{i=1}^n \log \frac{1}{1 + \exp(f(y_i))} \\
&= \sup_D \frac{1}{n} \sum_{i=1}^n \log(D(x_i)) + \sum_{i=1}^n \log(1 - D(y_i)).
\end{aligned}$$

Denote $F(D; Y) = \frac{1}{n} \sum_{i=1}^n \log(D(x_i)) + \sum_{i=1}^n \log(1 - D(y_i))$. Since $D(u) \in (0, 1)$ for any u, then $F(D; Y) \leq 0$. When $D(u) \to 0, \forall u$, we have $F(D; Y) \to -2 \log 2$, thus $\phi_{\mathrm{JS}}(Y, X) = \sup_D F(D; Y) \geq -2 \log 2$. Thus the range of $\phi_{\mathrm{JS}}(\cdot, \cdot)$ is $[-2 \log 2, 0]$.

Now we compute the value of $\phi_{\mathrm{JS}}(\cdot, X)$ for each Y. For any i, denote M_i to be set of indices of y_j such that y_j equals x_i, and m_i to be the size of the set M_i, i.e.,

$$M_i = \{j : y_j = x_i\}, m_i = |M_i|, i = 1, 2, \dots, n.$$

Denote $\Omega = \{1, 2, \dots, n\} \backslash (M_1 \cap M_2 \cdots \cap M_n)$. Then we have

$$\begin{aligned}
\phi_{\mathrm{JS}}(Y, X) =& \frac{1}{n} \sup_D \left(\sum_{i=1}^{n} [\log(D(x_i)) + \sum_{j \in M_i} \log(1 - D(y_j))] + \sum_{j \notin \Omega} \log(1 - D(y_j)) \right) \\
=& \frac{1}{n} \sup_D \left(\sum_{i=1}^{n} [\log(D(x_i)) + m_i \log(1 - D(x_i))] + \sum_{j \notin \Omega} \log(1 - D(y_j)) \right) \\
\overset{(i)}{=}& \frac{1}{n} \sum_{i=1}^{n} \sup_{t_i \in \mathbb{R}} [\log(t_i) + m_i \sum_{i=1}^{n} \log(1 - t_i)] + 0 \\
\overset{(ii)}{=}& \frac{1}{n} \sum_{i=1}^{n} [\log \frac{1}{m_i + 1} + m_i \log \frac{m_i}{m_i + 1}] \\
=& \frac{1}{n} \sum_{i=1}^{n} [m_i \log m_i - (m_i + 1) \log(m_i + 1)].
\end{aligned}$$

Here (i) is because $D(y_j), j \in \Omega$ are independent of $D(x_i)$'s and thus can be any values; in this step, the optimal $D(y_j) = 1, \forall j \in \Omega$. (ii) is because for any positive number m, $\sup_{t \in \mathbb{R}} [\log(t) + m \sum_{i=1}^{n} \log(1 - t)] = \log \frac{1}{m+1} + m \log \frac{m}{m+1}$.

When $m_i = 1, i = 1, 2, \dots, n$, i.e., $y_i = x_i, \forall i$, the function $\phi_{\mathrm{JS}}(Y, X)$ achieves value $-2 \log 2$. Thus $Y = (x_1, x_2, \dots, x_n)$ is a global minimum.

Next, we show that if Y satisfies that if $m_1 + m_2 + \cdots + m_n = n$ then Y is a strict local-min. Denote δ as the minimal distance between two points of $x_1, x_2, \dots, x_n$, i.e.,

$$\delta = \min_{k \neq l} \|x_k - x_l\|.$$

Consider a small perturbation of Y as $\bar{Y} = (\bar{y_1}, \bar{y_2}, \dots, \bar{y_n}) = (y_1 + \epsilon_1, y_2 + \epsilon_2, \dots, y_n + \epsilon_n)$, where $\|\epsilon_j\| < \delta, \forall j$ and $\sum_j \|\epsilon_j\|^2 > 0$. We want to verify that

$$\phi_{\mathrm{JS}}(\bar{Y}, X) > \phi_{\mathrm{JS}}(Y, X). \tag{11}$$

Denote

$$\bar{m}_i = |\{j : \bar{y}_j = x_i\}|, i = 1, 2, \dots, n.$$

According to the assumption $m_1 + m_2 + \cdots + m_n = n$, we have $y_j \in \{x_1, \dots, x_n\}, \forall j$. Consider an arbitrary j, and suppose $y_j = x_i$. Together with $\|\bar{y}_j - y_j\| = \|\epsilon_j\| < \delta = \min_{k \neq l} \|x_k - x_l\|$, we have $\bar{y}_j \notin (\{x_1, x_2, \dots, x_n\} \backslash \{x_i\})$. In other words, the only possible point in $\{x_1, \dots, x_n\}$ that can coincide with $\bar{y}_j$ is x_i, and this happens only when $\epsilon_j = 0$. As a result, we have

$$\bar{m}_i \leq m_i, \quad , i = 1, 2, \dots, n.$$

Together with the fact that $t \log t - (t + 1) \log(t + 1)$ is a strictly decreasing function in $t \in [0, \infty)$, we have

$$\begin{aligned}
\phi_{\mathrm{JS}}(\bar{Y}, X) &= \frac{1}{n} \sum_{i=1}^{n} [\bar{m}_i \log \bar{m}_i - (\bar{m}_i + 1) \log(\bar{m}_i + 1)] \\
&\geq \frac{1}{n} \sum_{i=1}^{n} [m_i \log m_i - (m_i + 1) \log(m_i + 1)] = \phi_{\mathrm{JS}}(Y, X).
\end{aligned}$$

The equality is achieved iff $\bar{m}_i = m_i, \forall i$, which holds iff $\epsilon_j = 0, \forall j$. Since we have assumed $\sum_j \|\epsilon_j\|^2 > 0$, the equality does not hold, thus $\phi(\bar{Y}, X) > \phi(Y, X)$. Therefore, we have proved that $\bar{Y}$ is a strict local minimum.

Finally, if Y satisfies that $m_1 + m_2 + \cdots + m_n = n$ and $m_k \geq 2$ for some k, then $\phi_{\mathrm{JS}}(Y, X) > -2 \log 2$. Thus Y is a sub-optimal strict local minimum. Q.E.D.

B Technical Details of Section 4.2 and 4.3

B.1 Proof of Claim 4.2

Define a function $\alpha_{ij}(t) = \frac{1}{2}\|y_i(t) - y_j(t)\|^2, \forall\, i, j.$

$$\begin{aligned}
\frac{d\alpha_{ij}(t)}{dt} &= (y_i - y_j)^T \frac{d(y_i - y_j)}{dt} = (y_i - y_j)^T \left(\frac{dy_i}{dt} - \frac{dy_j}{dt}\right) \\
&= (y_i - y_j)^T \left(\frac{w}{1 + e^{w^T y_i + b}} - \frac{w}{1 + e^{w^T y_j + b}}\right) \\
&= (w^T y_i - w^T y_j) \left(\frac{1}{1 + e^{w^T y_i + b}} - \frac{1}{1 + e^{w^T y_j + b}}\right) \\
&\leq 0.
\end{aligned}$$

In the last step, we used the fact that $(a_1 - a_2)\left(\frac{1}{1+e^{a_1}} - \frac{1}{1+e^{a_2}}\right) \leq 0$ for any $a_1, a_2 \in \mathbb{R}$. Note that in the above computation, we skip the time index t. Therefore $\alpha_{ij}(t)$ is non-increasing along the trajectory, which implies $\|y_i(t) - y_j(t)\| \leq \|y_i(0) - y_j(0)\|, \forall t$.

B.2 Proof of Claim 4.3

WGAN-GP with linear discriminators can be expressed as

$$\begin{aligned}
\min_{w \in \mathbb{R}^d} \; & L^D_{\mathrm{WGAN-GP}}(Y; \theta) \triangleq -\sum_{i=1}^n w^T x_i + \sum_{i=1}^n w^T y_i + \lambda(\|w\| - 1)^2. \\
\min_{Y=(y_1,\ldots,y_n) \in \mathbb{R}^{d \times n}} \; & L^G_{\mathrm{WGAN-GP}}(Y; \theta) \triangleq -\sum_{i=1}^n w^T y_i.
\end{aligned}$$

Consider the dynamics corresponding to the simultaneous gradient descent for WGAN-GP:

$$\frac{dw}{dt} = -\frac{\partial L^D_{\mathrm{WGAN-GP}}}{\partial w} = \sum_{i=1}^n (x_i - y_i) - 2\lambda w + 2w/\|w\|, \tag{12a}$$

$$\frac{dy_i}{dt} = -\frac{\partial L^G_{\mathrm{WGAN-GP}}}{\partial y_i} = -w. \tag{12b}$$

Define a function $\alpha_{ij}(t) = \frac{1}{2}\|y_i(t) - y_j(t)\|^2, \forall\, i, j.$

$$\begin{aligned}
\frac{d\alpha_{ij}(t)}{dt} &= (y_i - y_j)^T \frac{d(y_i - y_j)}{dt} = (y_i - y_j)^T \left(\frac{dy_i}{dt} - \frac{dy_j}{dt}\right) \\
&= (y_i - y_j)^T (w - w) \\
&= 0.
\end{aligned}$$

Thus $\|y_i(t) - y_j(t)\|$ will be a constant for all t.

C TECHNICAL DETAILS OF SECTION 4.2

C.1 PROOF OF CLAIM 4.2

Define a function $\alpha_{ij}(t) = \frac{1}{2}\|y_i(t) - y_j(t)\|^2, \forall\, i, j$.

$$\begin{aligned}
\frac{d\alpha_{ij}(t)}{dt} &= (y_i - y_j)^T \frac{d(y_i - y_j)}{dt} = (y_i - y_j)^T \left(\frac{dy_i}{dt} - \frac{dy_j}{dt}\right) \\
&= (y_i - y_j)^T \left(\frac{w}{1 + e^{w^T y_i + b}} - \frac{w}{1 + e^{w^T y_j + b}}\right) \\
&= (w^T y_i - w^T y_j) \left(\frac{1}{1 + e^{w^T y_i + b}} - \frac{1}{1 + e^{w^T y_j + b}}\right) \\
&\leq 0.
\end{aligned}$$

In the last step, we used the fact that $(a_1 - a_2)\left(\frac{1}{1+e^{a_1}} - \frac{1}{1+e^{a_2}}\right) \leq 0$ for any $a_1, a_2 \in \mathbb{R}$. Note that in the above computation, we skip the time index t. Therefore $\alpha_{ij}(t)$ is non-increasing along the trajectory, which implies $\|y_i(t) - y_j(t)\| \leq \|y_i(0) - y_j(0)\|, \forall t$.

C.2 PROOF OF CLAIM 5.1

Define a function $\alpha_{ij}(t) = \frac{1}{2}\|(y_i(t) - x_i) - (y_j(t) - x_j)\|^2, \forall\, i, j$. Denote $\delta_i(t) = y_i(t) - x_i$.

$$\begin{aligned}
\frac{d\alpha_{ij}(t)}{dt} &= (\delta_i - \delta_j)^T \frac{d(y_i - y_j)}{dt} = (\delta_i - \delta_j)^T \left(\frac{dy_i}{dt} - \frac{dy_j}{dt}\right) \\
&= (\delta_i - \delta_j)^T \left(\frac{w}{1 + e^{w^T(y_i - x_i)}} - \frac{w}{1 + e^{w^T(y_j - x_j)}}\right) \\
&= (w^T \delta_i - w^T \delta_j) \left(\frac{1}{1 + e^{w^T \delta_i}} - \frac{1}{1 + e^{w^T \delta_j}}\right) \\
&\leq 0.
\end{aligned}$$

The equality holds iff $w^T\delta_i = w^T\delta_j$, i.e., $w^T(\delta_i - \delta_j) = 0$.

C.3 PROOF OF CLAIM 5.2

Let $u_i = w^T(y_i - x_i), i = 1, \ldots, n$, we have

$$\frac{dV}{dt} = w^T \frac{dw}{dt} + \sum_i (y_i - x_i)^T \frac{dy_i}{dt} \tag{13a}$$

$$= w^T \sum_{i=1}^n \frac{x_i - y_i}{1 + e^{w^T(x_i - y_i)}} + \sum_i (y_i - x_i)^T \frac{w}{1 + e^{w^T(y_i - x_i)}} \tag{13b}$$

$$= \sum_{i=1}^n \frac{w^T(x_i - y_i)}{1 + e^{w^T(x_i - y_i)}} + \sum_{i=1}^n \frac{w^T(y_i - x_i)}{1 + e^{w^T(y_i - x_i)}} \tag{13c}$$

$$= \sum_{i=1}^n \frac{-u_i}{1 + e^{-u_i}} + \sum_{i=1}^n \frac{u_i}{1 + e^{u_i}} \tag{13d}$$

$$= \sum_{i=1}^n \sum_{i=1}^n \frac{u_i(1 - e^{u_i})}{1 + e^{u_i}} \leq 0, \tag{13e}$$

In the last step we used the fact that $u(1 - e^u) \leq 0,\ \forall u \in \mathbb{R}$. Note that in the above computation, we skip the time index t.

C.4 PROOF OF PROPOSITION 3

We restate the proposition below.

Proposition 4 *(restate; global convergence of CPGAN dynamics) When $d = 1$, starting from any initial point $\theta(0)$, the trajectory defined by the CPGAN dynamics $\theta(t)$ will satisfy $\lim_{t\to\infty} \theta(t) \in M$, where $M = \{(w, y) : w = 0, \sum_i x_i = \sum_i y_i\}$.*

We will use Lasalle's invariance principle (see, e.g. (Haddad & Chellaboina, 2011, Theorem 3.3) or (Cohen & Rouhling, 2017, Theorem 1)) to prove this result.

Definition (invariance set). A set A is said to be invariant with respect to a differential equation $\frac{du}{dt} = h(u(t))$ if every solution to this equation starting in A remains in A.

Lemma 1 *(Lasalle's invariance principle) Consider a dynamical system defined by $\frac{du}{dt} = h(u(t))$, where h is a vector mapping. Assume h has continuous first partial derivatives and $h(0) = 0$. Let K be an invariant compact set. Suppose there is a scalar function V which has continuous first partial derivatives in K and is such that $\tilde{V}(p) = \langle \nabla V(p), h(p)\rangle \leq 0, \forall p \in K$. Let E be the set of all points $p \in K$ such that $\tilde{V}(p) = 0$. Let M be the largest invariant set in E. Then for every solution t starting in K, $u(t) \to M$ as $t \to \infty$.*

Our goal is to show that starting from any initial point $\theta(0) = (w(0), y(0))$, the dynamics defined by (9), denoted as $\theta(t) = (w(t), y(t))$ will converge to the set

$$M = \{(w, y) : w = 0, \sum_i x_i = \sum_i y_i\}. \tag{14}$$

Define

$$K = \{\theta : \|\theta\|^2 \leq \|\theta(0)\|^2\}$$

Since $\dot{V} \leq 0$, we have $\|\theta(t)\|^2 \leq \|\theta(0)\|^2$, thus $\theta(t) \in K, \forall t$. Thus K is an invariant compact set.

According to Claim 5.2, the set of points p such that $\tilde{V}(p) = 0$ is

$$E \triangleq \{(w, y) : w^T(y_i - x_i) = 0, \forall i\}.$$

The analysis so far works for any d. Next, we will use the condition $d = 1$. We show that when M defined in (14) is the largest invariant set in E. Assume the contrary, that there is a set $M \subsetneq \bar{M} \subseteq E$ such that $\bar{M}$ is an invariant set. Then starting from any point $\theta(0) \in E\backslash M$, we have $\theta(t) \in \bar{M}$.

Since $d = 1$, then set E becomes

$$E = \{(w, y) \in \mathbb{R}^{1\times(n+1)} : w(y_i - x_i) = 0, \forall i\}.$$

Let $E_1 = \{(w, y) : w = 0\}$ and $E_2 = \{(w, y) : y_i = x_i, \forall i\}$, then $E = E_1 \cup E_2$. The set M is still

$$M = \{(w, y) : w = 0, \sum_i x_i = \sum_i y_i\}.$$

Since $\theta(0) \in E$ but not in M, and $E_2 \subseteq M$, then we have $\theta(0) \in E_1$ and $\theta(0) \notin E_2$. This implies $w(0) = 0$ and $\sum_i (x_i(0) - y_i(0))^2 \neq 0$. According to the fact that $\tilde{V}(p) = 0, \forall p \in E$ and $\theta(t) \in E$, we have that

$$V(\theta(t)) = V(\theta(0)) = \sum_i (x_i(0) - y_i(0))^2 + w(0)^2 \triangleq \delta. \tag{15}$$

Since the path $\theta(t) \in M \subseteq E$ for all t, we have $\theta(t) \in E_1$ or E_2. Suppose $J = \{t \in \mathbb{R} : \theta(t) \in E_2\}$, then for $s \in J$ we have $V(\theta(s)) = w(s)^2 + 0 = w(s)^2$. By (15), we have

$$w(s)^2 = \delta, \forall s.$$

For $t \notin J$, we have $\theta(t) \in E_1$ and thus $w(t) = 0$. Thus $w(t) = 0, \forall t \notin J$ and $w(t) = \delta, \forall s \in J$. As $w(t)$ is continuous for t and $w(0) = 0$, we must have $J = \emptyset$. This means $w(t) = 0$ for all t.

Recall the dynamics defined by 9 for the case $d = 1$ is

$$\frac{dw}{dt} = -\frac{\partial L^D_{\text{CP}}}{\partial w} = \sum_{i=1}^n \frac{x_i - y_i}{1 + e^{w(x_i - y_i)}}. \tag{16a}$$

$$\frac{dy_i}{dt} = -\frac{\partial L^G_{\text{CP}}}{\partial y_i} = \frac{w}{1 + e^{w(y_i - x_i)}}. \tag{16b}$$

Along the path $\theta(t) \in E$, we have $w(t)(y_i(t) - x_i(t)) = 0, \forall t$, thus

$$\frac{dy_i(t)}{dt} = \frac{0}{1 + e^0} = 0, \quad \forall i,$$

which implies $y_i(t) = y_i(0), \forall i$. This further implies $\frac{dw(t)}{dt} = \sum_i [x_i(t) - y_i(t)] = \sum_i [x_i(0) - y_i(0)] \triangleq \delta_0$. Since $\theta(0) \in E$ but not in M, thus we must have $\sum_i x_i(0) \neq \sum_i y_i(0)$, implying $\delta_0 \neq 0$. Thus $\frac{dw(t)}{dt} = \delta_0 \neq 0$, which contradicts $w(t) = 0, \forall t$. This contradiction implies that the original assumption that there is a set $M \subsetneq \bar{M} \subseteq E$ such that $\bar{M}$ is an invariant set does not hold. Thus the largest invariant subset of E must be a subset of M.

Finally, if $\theta(0) \in M$, then the gradients are zero, thus $\theta(t) \in M, \forall t$, which implies that M itself is a invariant set. Thus M is indeed the largest invariant set of E.

C.5 Proof of Claim 5.3

We restate the claim below.

Claim C.1 *When $d = 1$, for the training dynamics of (9), at any point other than the desired solution $(y_1, \dots, y_n) = (x_1, \dots, x_n)$ in the set of stationary solutions, the Jacobian has an eigenvalue with positive real part* [3].

When $d = 1$, the dynamical system is given by

$$\frac{dw}{dt} = -\frac{\partial L_{\mathrm{CP}}^D}{\partial w} = \sum_{i=1}^n \frac{x_i - y_i}{1 + e^{w(x_i - y_i)}}. \tag{17a}$$

$$\frac{dy_i}{dt} = -\frac{\partial L_{\mathrm{CP}}^G}{\partial y_i} = \frac{w}{1 + e^{w(y_i - x_i)}}. \tag{17b}$$

We can write it as

$$\dot{\theta} = h(\theta) = (h_0(\theta), \dots, h_n(\theta)),$$

where h_i is the right hand side of the i-th equation. The Jacobian $J = \nabla h$ satisfies the following:

$$\begin{aligned}
J_{11} &= \frac{\partial h_0}{\partial w} = \sum_{i=1}^n \frac{(x_i - y_i)^2}{1 + e^{w(y_i - x_i)}}, \\
J_{1,i+1} &= \frac{\partial h_0}{\partial y_i} = -\frac{1}{1 + e^{w(x_i - y_i)}} + w(x_i - y_i)\frac{e^{w(y_i - x_i)}}{(1 + e^{w(y_i - x_i)})^2}, \forall i = 1, \dots, n, \\
J_{i+1,1} &= \frac{\partial h_i}{\partial w} = \frac{1}{1 + e^{w(y_i - x_i)}} + w(y_i - x_i)\frac{e^{w(y_i - x_i)}}{(1 + e^{w(y_i - x_i)})^2}, \\
J_{i+1,i+1} &== \frac{\partial h_i}{\partial y_i} = -\frac{w^2 e^{w(y_i - x_i)}}{(1 + e^{w(y_i - x_i)})^2} \\
J_{ij} &= 0, \text{ if } i, j \geq 2 \text{ and } i \neq j.
\end{aligned}$$

When evaluated at $\theta = (0, y_1, \dots, y_n)$, we have

$$\begin{aligned}
J_{11} &= \sum_{i=1}^n \frac{(x_i - y_i)^2}{2}, \\
J_{1,i+1} &= -\frac{1}{2}, \forall i = 1, \dots, n, \\
J_{i+1,1} &= \frac{1}{2}, \\
J_{i+1,j+1} &= 0, \quad i, j \geq 1.
\end{aligned}$$

[3]The stability of typical equilibria of smooth ODEs is determined by the sign of real part of eigenvalues of the Jacobian matrix. It is unstable if at least one eigenvalue has positive real part. See, e.g., Mescheder (2018) for the discussions.

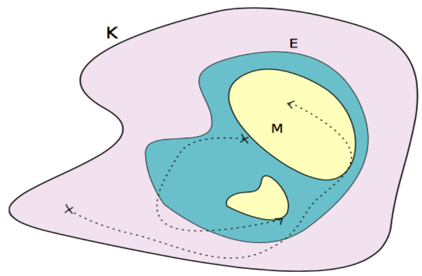

Figure 4: Graphical illustration of LaSalle's invariance principle. Figure from Cohen & Rouhling (2017). Starting from K, the dynamics will finally converge to the set M.

It is easy to verify that J only has two non-zero eigenvalues

$$\lambda_{1,2} = \frac{1}{2} J_{11} \pm \frac{1}{\sqrt{2}} \sqrt{-1}.$$

Therefore, when $x_i = y_i, \forall x_i$, the eigenvalues of the Jacobian have zero real part. When some $x_i \neq y_i$, then the two eigenvalues of the Jacobian have negative real part, meaning that this stationary point is not stable. This proves the result: in the set of stationary solutions $M = \{(w, y) : w = 0, \sum_i x_i = \sum_i y_i\}$, any point other than the desired solution $(y_1, \dots, y_n)$ is not stable.

D Proof of Proposition 2 for $n = 2$

Without loss of generality, we can consider two points $x_1 = 0, x_2 = 1$. The problem becomes

$$g^{\mathrm{CP}}(Y) = \sup_{f \in \mathcal{F}} \frac{1}{2} \log \frac{1}{1 + \exp(f(0) - f(y_1))} + \frac{1}{2} \log \frac{1}{1 + \exp(f(1) - f(y_2))},$$

where $\mathcal{F}$ is the set of continuous functions with domain $\mathbb{R}^d$. We compute all values of $g^{\mathrm{CP}}(Y)$ as follows.

Case 1: The two generated points are the same as the true data points, i.e., $\{x_1, x_2\} = \{y_1, y_2\}$. If $y_1 = 0, y_2 = 1$, then

$$g^{\mathrm{CP}}(Y) = \frac{1}{2} [\log 1/2 + \log 1/2] = -\log 2 \approx -0.6937.$$

If $y_1 = 1, y_2 = 0$, then

$$\begin{aligned} g^{\mathrm{CP}}(Y) &= \sup_{f \in \mathcal{F}} \left[\frac{1}{2} \log \frac{1}{1 + \exp(f(0) - f(1))} + \frac{1}{2} \log \frac{1}{1 + \exp(f(1) - f(0))} \right] \\ &= \sup_{t \in \mathbb{R}} \left[\frac{1}{2} \log \frac{1}{1 + \exp(t)} + \frac{1}{2} \log \frac{1}{1 + \exp(-t)} \right] \\ &= -\log 2. \end{aligned}$$

Case 2: Exactly one of the generated points coincides with the corresponding true data point, i.e., $|\{i : y_i = x_i\}| = 1$. Without loss of generality, we can check the case $y_1 = 0, y_2 \neq 1$. Then

$$\begin{aligned} g^{\mathrm{CP}}(Y) &\geq \sup_{f \in \mathcal{F}} \frac{1}{2} \log \frac{1}{1 + \exp(f(0) - f(0))} + \frac{1}{2} \log \frac{1}{1 + \exp(f(1) - f(y_2))} \\ &= -\frac{1}{2} \log 2 + \sup_{t \in \mathbb{R}} \frac{1}{2} \log \frac{1}{1 + \exp(t)} \\ &= -\frac{1}{2} \log 2 \approx -0.3466. \end{aligned}$$

The value is achieved when $f(1) - f(y_2) \to -\infty$ (or more precisely, there is a sequence of functions such that the difference $f(1) - f(y_2)$ goes to minus infinity).

Case 3: Both generated points are different from the true data points, i.e., $|\{i : y_i = x_i\}| = 1$. Then

$$\begin{aligned} g^{\mathrm{CP}}(Y) &\geq \sup_{f \in \mathcal{F}} \frac{1}{2} \log \frac{1}{1 + \exp(f(0) - f(y_1))} + \frac{1}{2} \log \frac{1}{1 + \exp(f(1) - f(y_2))} \\ &= \sup_{t_1 \in \mathbb{R}, t_2 \in \mathbb{R}} \frac{1}{2} \log \frac{1}{1 + \exp(t_1)} + \frac{1}{2} \log \frac{1}{1 + \exp(t_2)} \\ &= 0. \end{aligned}$$

The value is achieved when $f(1) - f(y_2) \to -\infty$ and $f(0) - f(y_2) \to -\infty$.

According to the above results, the only global minima are $\{y_1, y_2\} = \{x_1, x_2\}$. In addition, from any Y, it is easy to verify that there is a non-decreasing path from Y to a global minimum.

E PROOF OF PROPOSITION 2 FOR GENERAL n

Recall the function

$$g(Y) = \sup_f \frac{1}{n} \sum_{i=1}^{n} \log \frac{1}{1 + \exp(f(y_i) - f(x_i)))} = -\inf_f \frac{1}{n} \sum_{i=1}^{n} \log\left(1 + \exp(f(y_i) - f(x_i))\right).$$

Proposition 5 *(restatement of Proposition 2) Suppose $x_1, x_2, \ldots, x_n \in \mathbb{R}^d$ are distinct. The global minimal value of $g^{\mathrm{CP}}(Y)$ is $-\log 2$, which is achieved iff $\{x_1, \ldots, x_n\} = \{y_1, \ldots, y_n\}$. Furthermore, the function $g(Y)$ has no sub-optimal basin.*

The key of the proof is to compute the values of $g(Y)$ for any Y. Roughly speaking, the value $g(Y)$ can be computed by the following process:

(1) We can build a graph with vertices representing distinct values in $x_i's, y_i's$ and draw directed edges from x_i to y_i. This graph can be decomposed into cycles and trees.

(2) Each vertex in a cycle contributes $-\frac{1}{n}\log 2$ to the value $g(Y)$.

(3) Each vertex in a tree contributes 0 to the value $g(Y)$.

Putting these ideas together, the value $g(Y)$ equals $-\frac{1}{n}\log 2$ times the number of vertices in the cycles.

The outline of this section is as follows. In the first subsection, as a warm-up example, we prove that if $\{y_1, y_2, \ldots, y_n\} = \{x_1, \ldots, x_n\}$, then Y is a global minimum of $g(Y)$. In the second subsection, as another warm-up example, we prove that if there exists some $y_i \notin \{x_1, \ldots, x_n\}$, then it is not a global minimum. In the third subsection, we prove Proposition 2, in three steps. The proofs of some technical lemmas will be provided in the remaining subsections.

E.1 WARM-UP EXAMPLE 1: ALL GENERATED POINTS MATCH THE TRUE POINTS

Prove that if $\{y_1, y_2, \ldots, y_n\} = \{x_1, \ldots, x_n\}$, then Y is a global minimum of $g(Y)$.

Suppose $y_i = x_{\sigma(i)}$, then $(\sigma(1), \sigma(2), \ldots, \sigma(n))$ is a permutation of $(1, 2, \ldots, n)$. We view σ as a mapping from $\{1, 2, \ldots, n\}$ to $\{1, 2, \ldots, n\}$. Pick an arbitrary i, then in the infinite sequence $i, \sigma(i), \sigma(\sigma(i)), \sigma^{(3)}(i), \ldots$ there exists at least two numbers that are the same. Suppose $\sigma^{(k_0)}(i) = \sigma^{(k_0+T)}(i)$ for some k_0, T, then since σ is a one-to-one mapping we have $i = \sigma^{(T)}(i)$. Then we obtain a cycle $C = (i, \sigma(i), \sigma^{(2)}(i), \ldots, \sigma^{(T-1)}(i))$.

We can divide $\{1, 2, \ldots, n\}$ into the collection of finitely many cycles $C_1, C_2, \ldots, C_K$. Each cycle $C_k = (c_k(1), c_k(2), \ldots, c_k(m_k))$ satisfies $c_k(j+1) = \sigma(c_k(j)), j = 1, 2, \ldots, m_k$ where $c_k(m_k +$

1) is defined as $c_k(1)$. Now we calculate the value of $g(Y)$.

$$
\begin{aligned}
g(Y) &= \sup_f \frac{1}{n}\sum_{i=1}^{n} \log \frac{1}{1+\exp(f(y_i)-f(x_i)))} \\
&\overset{\text{(i)}}{=} -\inf_f \frac{1}{n}\sum_{k=1}^{K}\sum_{i\in C_k} \log\left(1+\exp(f(y_i)-f(x_i))\right)) \\
&= -\inf_f \frac{1}{n}\sum_{k=1}^{K}\sum_{j=1}^{m_k} \log\left(1+\exp(f(x_{c_k(j+1)})-f(x_{c_k(j)}))\right)) \\
&\overset{\text{(ii)}}{=} -\frac{1}{n}\sum_{k=1}^{K}\inf_f\sum_{j=1}^{m_k} \log\left(1+\exp(f(x_{c_k(j+1)})-f(x_{c_k(j)}))\right)) \\
&= -\frac{1}{n}\sum_{k=1}^{K}\inf_{t_1,t_2,\ldots,t_{m_k}\in\mathbb{R}}\left[\sum_{j=1}^{m_k-1}\log\left(1+\exp(t_{j+1}-t_j)\right)+\log\left(1+\exp(t_1-t_{m_k})\right)\right] \\
&\overset{\text{(iii)}}{=} -\frac{1}{n}\sum_{k=1}^{K} m_k\log(1+\exp(0)) \\
&= -\log 2.
\end{aligned}
$$

Here (i) is because $\{1,2,\ldots,n\}$ is the combination of $C_1,\ldots,C_K$ and $i\in C_k$ means that $i=c_k(j)$ for some j. (ii) is because C_k's are disjoint and f can be any continuous function; more specifically, the values of f at x_i's for i in two different cycles are independent, i.e., the choice of $\{f(x_i): i\in C_{k_1}\}$ is independent of the choice of $\{f(x_i): i\in C_{k_2}\}$ if $k_1\neq k_2$, thus we can take the infimum over each cycle (i.e. put "inf" inside the sum over k). (iii) is because $\sum_{j=1}^{m-1}\log(1+\exp(t_{j+1}-t_j))+\log\left(1+\exp(t_1-t_m)\right)$ is a convex function of $t_1,t_2,\ldots,t_m$ and the minimum is achieved at $t_1=t_2=\ldots t_m=0$.

E.2 Warm-up example 2: new point generated

Suppose $y_j\in\{x_1,\ldots,x_n\},\forall j$, and there exist some x_{i_0} that is not equal to any y_j. In this part, we compute the value $g(Y)$ and show that Y is not a global minimum. The computation for this example will illustrate how a "free" variable reduces the objective value $g(Y)$ by at least $-\frac{1}{n}\log 2$. Later in the general proof, we will see that any vertex not in a cycle will reduce the objective value by exactly $-\frac{1}{n}\log 2$.

Consider the term $\log(1+\exp(f(y_{i_0})-f(x_{i_0})))$. Since x_{i_0} does not appear in any other term in $\sum_i\log(1+\exp(f(y_i)-f(x_i)))$, the choice of $f(x_{i_0})$ is free. Therefore, no matter what values of $f(x_1),\ldots,f(x_{i_0-1}),f(x_{i_0+1}),\ldots,f(x_n)$ and $f(y_1),\ldots,f(y_n)$ are, we can always pick $f(x_{i_0})$ so that $f(y_{i_0})-f(x_{i_0})\to-\infty$, making the term $\log(1+\exp(f(y_{i_0})-f(x_{i_0})))\to 0$.

$$
\begin{aligned}
g(Y) &= -\inf_f \frac{1}{n}\sum_{i=1}^{n}\log\left(1+\exp(f(y_i)-f(x_i))\right)) \\
&= -\inf_f \frac{1}{n}\sum_{i\neq i_0}\log\left(1+\exp(f(y_i)-f(x_i))\right))+0 \\
&\geq -\frac{1}{n}\sum_{i\neq i_0}\log(1+1) \\
&= -\frac{n-1}{n}\log 2.
\end{aligned}
$$

E.3 Formal proof of Proposition 2

This proof is divided into three steps. In Step 1, we compute the value of $g(Y)$ if all $y_i\in\{x_1,\ldots,x_n\}$. This is the major step of the whole proof. In Step 2, we compute the value of $g(Y)$

for any Y. In Step 3, we show that if Y is not a global minimum, then there is a non-decreasing continuous path from Y to a global minimum.

E.3.1 Step 1: Compute $g(Y)$ that all $y_i \in \{x_1, \dots, x_n\}$

Assume

$$y_i \in \{x_1, \dots, x_n\}, \forall i. \tag{18}$$

We build a directed graph $G = (V, A)$ as follows. The set of vertices $V = \{1, 2, \dots, n\}$ represents $x_1, x_2, \dots, x_n$. We draw a directed edge $(i, j) \in A$ if $y_i = x_j$; in this case, there is a term $\log(1 + \exp(f(x_j) - f(x_i)))$ in the expression of $g(Y)$. Note that in this directed graph, it is possible to have a self-loop (i, i), which corresponds to the case $y_i = x_i$. Because of the assumption (18), we can simply express

$$\begin{aligned} g(Y) &= -\inf_f \frac{1}{n} \sum_{i=1}^{n} \log\left(1 + \exp(f(y_i) - f(x_i))\right) \\ &= -\inf_f \frac{1}{n} \sum_{(i,j) \in A} \log\left(1 + \exp(f(x_j) - f(x_i))\right). \end{aligned} \tag{19}$$

Each y_i correspond to a unique x_j, thus the outdegree of i, denoted as outdegree(i), must be exactly 1; in other words, for each i there is exactly one directed edge going out from i. The indegree of each i, denoted as indegree(i), can be any number in $\{0, 1, \dots, n\}$.

To proceed, we need a few definitions from standard graph theory.

Definition E.1 *(walk, path and cycle) In a directed graph G, a directed walk (or more simply, walk) $W = (v_0, e_1, v_1, e_2, \dots, v_{m-1}, e_m, v_m)$ is a sequence of vertices and edges such that $v_i \in V$ for every $i \in \{0, 1, \dots, m\}$ and e_i is a directed edge from v_{i-1} to v_i for every $i \in \{1, \dots, m\}$. The set of vertices in W is denoted as $V(W)$, and the set of edged in W is denoted as $A(W)$. If $v_0, v_1, \dots, v_m$ are distinct we call it a directed path (or path), and we say the length of the path is m. If $v_0, v_1, \dots, v_{m-1}$ are distinct and $v_m = v_0$, we call it a directed cycle (or cycle).*

Note that we always say v has a path to itself v (with length 0), no matter whether there is an edge between v to itself or not. This is because the degenerate walk $W = (v)$ satisfies the conditions of the above definition.

Definition E.2 *(tree) A directed tree is a directed graph $T = (V, A)$ with a designated node $r \in V$, the root, such that there is exactly one path from v to r for each node $v \in V$ and there is no edge from the root r to itself. The depth of a node in a tree is the length of the path from the node to the root (define the depth of the root to be 0). A subtree of a directed graph G is a subgraph T of $G = (V, A)$ which is a directed tree. The set of vertices in T is denoted as $V(T)$, and the set of edged in T is denoted as $A(T)$.*

We prove a lemma that states that the graph can be decomposed into the union of cycles and trees. A graphical illustration is given in Figure 6.

Lemma 2 *Suppose $G = (V, A)$ is a directed graph and outdegree$(v) = 1, \forall v \in V$. Then we have the following:*

(a) There exist cycles $C_1, C_2, \dots, C_K$ and subtrees $T_1, T_2, \dots, T_M$ such that each edge $v \in A$ appears either in exactly one of the cycles or in exactly one of the subtrees.

(b) The root of each subtree u_m is a vertex of a certain cycle C_k where $1 \leq k \leq K$. In addition, each vertex of the graph appears in exactly one of the following sets: $V(C_1), \dots, V(C_K), V(T_1)\backslash\{u_1\}, \dots, V(T_M)\backslash\{u_M\}$,

(c) There is at least one cycle in the graph;

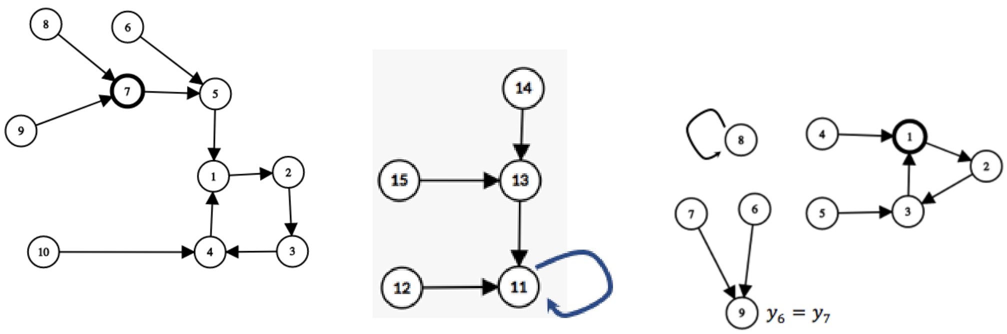

(a) Example 1 for Lemma 2 (b) Example 2 for Lemma 2, with self-loop (c) Example for Lemma 3

Figure 5: The first figure is a connected component of a graph. It contains 10 vertices and 10 directed edges. It can be decomposed into a cycle and two subtrees. The cycle consists of vertices $1, 2, 3, 4$. The first subtree consists of edge $(10, 4)$ and vertices $10, 4$, and the second subtree consists of edges $(8, 7), (9, 7), (7, 5), (6, 5), (5, 1)$. The second figure is another connected component of the same graph as the first figure. It has one cycle being a self-loop, and two trees attached to it. The third figure is an example of Lemma 3. There is one vertice 9 with outdegree 0, which corresponds to y_6 and y_7 since both 6 and 7 are connected to it. The fact that the two edges have the same head 9 implies that $y_6 = y_7$.

With this lemma, we are ready to compute the value $g(Y)$. According to Lemma 2, we have

$$
\begin{aligned}
&- ng(Y) = \inf_f \sum_{i=1}^{n} \log\left(1 + \exp(f(y_i) - f(x_i))\right)\\
&= \inf_f \left[\sum_{k=1}^{K} \sum_{i \in V(C_k)} \log\left(1 + \exp(f(y_i) - f(x_i))\right) + \sum_{m=1}^{M} \sum_{i \in V(T_m) \backslash \{u_m\}} \log\left(1 + \exp(f(y_i) - f(x_i))\right) \right]\\
&\geq \inf_f \left[\sum_{k=1}^{K} \sum_{i \in V(C_k)} \log\left(1 + \exp(f(y_i) - f(x_i))\right) \right] \triangleq g_{\text{cyc}}.
\end{aligned} \tag{20}
$$

We then compute g_{cyc}. Since C_k is a cycle, we have $X_k \triangleq \{x_i : i \in C_k\} = \{y_i : i \in C_k\}$. Since the cycles C_k's are disjoint, we have $X_k \cap X_l = \emptyset, \forall k \neq l$, meaning that the values $f(x_i), f(y_i)$ for i in one cycle C_k are independent of the values corresponding to a different cycle C_l. Then the sum in the expression of g_{cyc} can be decomposed according to different cycles.

$$
\begin{aligned}
g_{\text{cyc}} &= \inf_f \left[\sum_{k=1}^{K} \sum_{i \in V(C_k)} \log\left(1 + \exp(f(y_i) - f(x_i))\right) \right]\\
&= \sum_{k=1}^{K} \inf_f \sum_{i \in V(C_k)} \log\left(1 + \exp(f(y_i) - f(x_i))\right)
\end{aligned}
$$

Similar to Step 1, we can show that the infimum for each cycle is achieved when the values $f(x_i) = f(x_j), \forall i, j \in V(C_k)$. A more detailed proof is given as follows. Pick an arbitrary k, and suppose all the edges of C_k are $(v_1, v_2), (v_2, v_3), \ldots, (v_{r-1}, v_r), (v_r, v_1)$, where $r = |V(C_k)|$ is the number of vertices in the cycle C_k. Denote $v_{r+1} = v_1$. Then

$$\begin{aligned}
&\inf_f \sum_{i \in V(C_k)} \log\left(1 + \exp(f(y_i) - f(x_i))\right)\\
=&\inf_f \sum_{j=1}^{r} \log\left(1 + \exp(f(x_{v_{j+1}}) - f(x_{v_j}))\right)\\
=&\inf_{t_1, t_2, \ldots, t_r \in \mathbb{R}} \left[\sum_{j=1}^{r-1} \log\left(1 + \exp(t_{j+1} - t_j)\right) + \log\left(1 + \exp(t_1 - t_r)\right)\right]\\
=&r \log 2 = |V(C_k)| \log 2.
\end{aligned} \tag{21}$$

The infimum is achieved when $f(x_{v_1}) = \cdots = f(x_{v_r})$, or equivalently, $f(x_i) = f(x_j), \forall i, j \in V(C_k)$. Therefore,

$$g_{\text{cyc}} = \log 2 \sum_{k=1}^{K} |V(C_k)|. \tag{22}$$

According to (20) and (22), we have

$$-ng(Y) \geq \sum_{k=1}^{K} |V(C_k)| \log 2. \tag{23}$$

Next, we prove that for any $\epsilon > 0$, there exists a continuous function f such that

$$-ng(Y) < \sum_{k=1}^{K} |V(C_k)| \log 2 + \epsilon. \tag{24}$$

Let N be a large positive number such that

$$n \log\left(1 + \exp(-N)\right) < \epsilon. \tag{25}$$

Pick a continuous function f as follows.

$$f(x_i) = \begin{cases} 0, & i \in \bigcup_{k=1}^{K} V(C_k), \\ N \cdot \text{depth}(i), & i \in \bigcup_{m=1}^{M} V(T_m). \end{cases} \tag{26}$$

Note that the root u_m of a tree T_m is also in a certain cycle C_k, thus the value $f(x_{u_m})$ is defined twice in (26), but in both definitions its value is 0, thus the definition is valid. For any $i \in V(C_k)$, suppose $y_i = x_j$, then both $i, j \in V(C_k)$ which implies $f(y_i) - f(x_i) = f(x_j) - f(x_i) = 0$. For any $i \in V(T_m) \backslash \{u_m\}$, suppose $y_i = x_j$, then by the definition of the graph (i, j) is a directed edge of the tree T_m, which means that depth(i) = depth(j)+1. Thus $f(y_i) - f(x_i) = f(x_j) - f(x_i) = -N$. In summary, for the choice of f in (26), we have

$$f(y_i) - f(x_i) = \begin{cases} 0, & i \in \bigcup_{k=1}^{K} V(C_k), \\ -N, & i \in \bigcup_{m=1}^{M} V(T_m). \end{cases} \tag{27}$$

For the choice of f in (26), we have

$$
\begin{aligned}
&-nF(Y;f)\\
=&\sum_{i=1}^{n}\log\left(1+\exp(f(y_i)-f(x_i))\right)\\
=&\left[\sum_{k=1}^{K}\sum_{i\in V(C_k)}\log\left(1+\exp(f(y_i)-f(x_i))\right)+\sum_{m=1}^{M}\sum_{i\in V(T_m)\backslash\{u_m\}}\log\left(1+\exp(f(y_i)-f(x_i))\right)\right]\\
\overset{(27)}{=}&\left[\sum_{k=1}^{K}\sum_{i\in V(C_k)}\log\left(1+\exp(0)\right)+\sum_{m=1}^{M}\sum_{i\in V(T_m)\backslash\{u_m\}}\log\left(1+\exp(-N)\right)\right]\\
=&\sum_{k=1}^{K}|V(C_k)|\log 2+\sum_{k=1}^{M}(|V(T_m)|-1)\log\left(1+\exp(-N)\right)\\
\le&\sum_{k=1}^{K}|V(C_k)|\log 2+n\log\left(1+\exp(-N)\right)\\
\overset{(25)}{<}&\sum_{k=1}^{K}|V(C_k)|\log 2+\epsilon.
\end{aligned}
$$

This proves (24).

Combining (23) and (24), we have $-ng(Y)=\sum_{k=1}^{K}|V(C_k)|\log 2$, or equivalently,

$$g(Y)=\frac{1}{n}\sum_{k=1}^{K}|V(C_k)|\log 2.$$

E.3.2 STEP 2: COMPUTE $g(Y)$ FOR ANY Y

In the general case, not all y_i's lie in the set $\{x_1,\dots,x_n\}$. Denote the set

$$H=\{i: y_i\in\{x_1,\dots,x_n\}\},\quad H^c=\{j: y_j\notin\{x_1,\dots,x_n\}\}.$$

Since y_j's in H^c may be the same, we define the set of such distinct values of y_j's as

$$Y_{\text{out}}=\{y\in\mathbb{R}^d: y=y_j,\ \text{for some } j\in H^c\}.$$

Let $n_{\text{out}}=|Y_{\text{out}}|$, then there are total $n+n_{\text{out}}$ distinct values in $x_1,\dots,x_n,y_1,\dots,y_n$. Without loss of generality, assume $y_1,\dots,y_{n_{\text{out}}}$ are distinct (this is because the value of $g(Y)$ does not change if we re-index x_i's and y_i's as long as the subscripts of x_i,y_i change together), then

$$Y_{\text{out}}=\{y_1,\dots,y_{n_{\text{out}}}\}.$$

We build a directed graph $G=(V,A)$ as follows. The set of vertices $V=\{1,2,\dots,n,n+1,\dots,n+n_{\text{out}}\}$ represents $x_1,x_2,\dots,x_n$ and $y_1,\dots,y_{n_{\text{out}}}$. For $i,j\le n$, we draw a directed edge $(i,j)\in A$ if $y_i=x_j$; in this case, there is a term $\log(1+\exp(f(x_j)-f(x_i)))$ in the expression of $g(Y)$. For $1\le i\le n$ and $1\le j\le n_{\text{out}}$, we draw a directed edge $(i,n+j)\in A$ if $y_i=y_j$; in this case, there is a term $\log(1+\exp(f(y_j)-f(x_i)))$ in the expression of $g(Y)$. Note that in this directed graph, it is possible to have a self-loop (i,i), which corresponds to the case $y_i=x_i$.

This graph has the following property: for each $1\le i\le n$, the outdegree is exactly 1; for each $n\le j\le n+n_{\text{out}}$, the outdegree of j is 0. Moreover, each vertex representing some y_i has an incoming degree at least 1 (since otherwise this vertex will not be created); note that an vertex representing x_i may have incoming degree 0. We present a lemma which is an extension of the Lemma 2. The proof is given in Appendix E.5.

Lemma 3 *Suppose $G=(V,A)$ is a directed graph and outdegree$(v)\le 1,\forall v\in V$. Then we have the following:*

(a) There exist cycles $C_1, C_2, \ldots, C_K$ and subtrees $T_1, T_2, \ldots, T_M$ such that each edge $v \in A$ appears either in exactly one of the cycles or in exactly one of the subtrees.

(b) Denote the root of subtree T_m as u_m, $m = 1, \ldots, M$. Then u_m is either a vertex of a certain cycle C_k where $1 \leq k \leq K$, or a vertex with outdegree 0.

(c) Suppose $u_1, \ldots, u_{M_0}$ are in a certain cycle, and $u_{M_0+1}, \ldots, u_M$ have outdegree 0. Then each vertex of the graph appears in exactly one of the following sets: $V(C_1), \ldots, V(C_K), V(T_1)\backslash\{u_1\}, \ldots, V(T_{M_0})\backslash\{u_{M_0}\}, V(T_{M_0+1}), \ldots, V(T_M)$.

Note that (b) is different from Lemma 2, because under the assumption of that lemma that each vertex has an outgoing edge, the root of a tree cannot have outdegree 0.

The computation of $g(Y)$ is quite similar to the previous case. We will highlight a few small differences. We still have

$$\begin{aligned}
& - ng(Y) \\
=& \inf_f \sum_{i=1}^{n} \xi(f(y_i) - f(x_i)) \\
=& \inf_f \left[\sum_{k=1}^{K} \sum_{i \in V(C_k)} \xi(f(y_i) - f(x_i)) + \sum_{m=1}^{M} \sum_{i \in V(T_m)\backslash\{u_m\}} \xi(f(y_i) - f(x_i) \right] \\
\geq& \inf_f \left[\sum_{k=1}^{K} \sum_{i \in V(C_k)} \log\left(1 + \exp(f(y_i) - f(x_i))\right) \right] \\
\triangleq& g_{\text{cyc}}.
\end{aligned} \tag{28}$$

Same as before, we have $g_{\text{cyc}} = \sum_{k=1}^{K} |V(C_k)| \log 2$. Once we fix the values of $f(x_i)$ to be a constant for i in cycles (which makes the first sum achieves the value $\sum_{k=1}^{K} |V(C_k)| \log 2$), we can always pick the values of f on the vertices j in the trees so that $f(y_j) - f(x_j) \to \infty$. Therefore, we have

$$-ng(Y) = g_{\text{cyc}} = \sum_{k=1}^{K} |V(C_k)| \log 2.$$

E.3.3 Step 3: Finding a non-decreasing path to a global minimum

Finally, we prove that for any Y, there is a non-decreasing continuous path from Y to one global minimum Y^*. In other words, there is a continuous function $\eta : [0, 1] \to \mathbb{R}^{d \times n}$ such that $\eta(0) = \bar{Y}, \eta(1) = Y^*$ and $g(\eta(t))$ is a non-decreasing function with respect to $t \in [0, 1]$. In this proof, we will just describe the path in words, and skip the rigorous definition of the continuous function η, since it should be clear from the context how to define η.

The following claim shows that we can increase the value of Y incrementally; see the proof in Appendix E.6

Claim E.1 *For an arbitrary Y that is not a global minimum, there exists another $\hat{Y}$ and a non-decreasing continuous path from Y to $\hat{Y}$ such that $g(\hat{Y}) - g(Y) \geq \frac{1}{n} \log 2$.*

For any Y that is not a global minimum, we apply Claim E.1 for finitely many times (no more than n times), then we will arrive at one global minimum Y^*. We connect all non-decreasing continuous paths, and get a non-decreasing continuous path from Y to Y^*. This finishes the proof of Proposition 2.

E.4 Proof of Lemma 2

We first prove a few observations. We will slightly extend the definition of "walk" to allow a walk with infinite length.

Observation 1: Suppose in a directed graph $G = (V, A)$, any vertex has outdegree exactly 1. Starting from any vertex $v_0 \in V(G)$, there is a unique walk with infinite length

$$W(v_0) \triangleq (v_0, e_1, v_1, e_2, v_2, \dots, v_i, e_i, v_{i+1}, e_{i+1}, \dots),$$

where e_i is an edge in $A(G)$ with tail v_{i-1} and head v_i.

Proof of Observation 1: At each vertex v_i, there is a unique outgoing edge $e_i = (v_i, v_{i+1})$ which uniquely defines the next vertex v_{i+1}. Continue the process, we have proved Observation 1. □

Observation 2: Suppose in a directed graph $G = (V, A)$, any vertex has outdegree exactly 1. Suppose the unique walk starting from v_0 is $W(v_0) \triangleq (v_0, e_1, v_1, e_2, v_2, \dots, v_i, e_i, v_{i+1}, e_{i+1}, \dots)$, then the walk can be decomposed into two parts

$$W_1(v_0) = (v_0, e_1, v_1, e_2, v_2, \dots, v_{i_0-1}, e_{i_1}, v_{i_0}),$$
$$W_2(v_0) = (v_{i_0}, e_{i_0+1}, v_{i_0+1}, e_{i_0+2}, v_{i_0+2}, \dots),$$

where $W_1(v_0)$ is a directed path from v_0 to v_{i_0} (i.e. the vertices $v_0, v_1, \dots, v_{i_0}$ are distinct), and $W_2(v_0)$ is the repetition of a certain cycle (i.e. there exists T such that $v_{i+T} = v_i$, for any $i \geq i_0$). This decomposition is unique.

Proof of Observation 2: Since there are only finitely many vertices in the graph, then some vertices must appear at least twice in $W(v_0)$. Among all such vertices, suppose u is the one that appears the earliest in the walk $W(v_0)$, and the first two appearances are $v_{i_0} = u$ and $v_{i_1} = u$ and $i_0 < i_1$. Denote $T = i_1 - i_0$. Since there is a unique edge going out from any vertex, thus v_{i_0+1} must be the same as $v_{i_1+1} = v_{i_0+1+T}$. Continue the process, we have $v_i = v_{i+T}$ for any $i \geq i_0$. Thus starting from $u = v_{i_0}$, the walk $W_2(v_0)$ will be repetitions of the cycle consisting of vertices $v_{i_0}, v_{i_0+1}, \dots, v_{i_1-1}$, and we denote this cycle as C_{k_0}.

If the vertices before v_{i_1} are not distinct, then there are at least two vertices $v_j = v_l$ where $0 \leq j < l \leq i_0$. This contradicts the definition of i_0. Therefore, $W_1(v_0)$ is a directed path from v_0 to v_{i_0}. □

In Observation 2, for any $v_0 \in V$, the "transition point" v_{i_0} in the infinite walk $W(v_0)$ is unique. We define the "first-touch-vertex" of v_0 to be v_{i_0}. The first-touch-vertex $u = v_{i_0}$ has the following properties: (i) $u \in C_k$ for some k; (ii) there exists a path from v to u; (iii) any paths from v to any vertex in the cycle C_k other than u must pass u. In other words, if an ant starts from v_0 and crawls along the edges, the first vertex in a cycle that it touches is u. Since any v_0 corresponds to a unique $W(v_0)$, its first-touch-vertex must exist and unique. Note that if u is in some cycle, then its first-touch-point is u itself.

As a corollary of Observation 2, there is at least one cycle in the graph. Suppose all cycles of G are $C_1, C_2, \dots, C_K$. Because the outdegree of each vertex is 1, these cycles must be disjoint, i.e., $V(C_i) \cap V(C_j) = \emptyset$ and $A(C_i) \cap A(C_j) = \emptyset$, for any $i \neq j$.

Define R to be the set of vertices of $C_1, \dots, C_m$ with indegree at least two, i.e.,

$$R \triangleq \{v : v \in C_k \text{ for some } k, \text{ and indegree}(v) \geq 2\}.$$

Suppose the elements of R are $u_1, \dots, u_M$. We denote the set of vertices in the cycles as

$$V_c = \bigcup_{k=1}^{K} V(C_1) \cup \dots \cup V(C_K). \tag{29}$$

We describe the intuition behind the partitioning of G. Based on Observation 2, starting from any vertex outside of V_c there is a unique path that reaches V_c. Combining all vertices that reach the cycles at u_m (denoted as V_m), and the paths from these vertices to u_m, we obtain a directed subgraph T_m, which is connected with V_c only via the vertex u_m. The subgraphs T_m's are disjoint from each other since they are connected with V_c via different vertices. In addition, each vertex outside of V_c lies in exactly one of the subgraph T_m. Thus, we can partition the whole graph into the union of the cycles $C_1, \dots, C_K$ and the subgraphs $T_1, \dots, T_M$.

Next, we provide more formal definitions and proofs. For any $m \in \{1, 2, \ldots, M\}$, define

$$\bar{V}_m = \{v \in V(G) : u_m \text{ is the first-touch-vertex of } v\}, \tag{30a}$$
$$V_m = \bar{V}_m \backslash \{u_m\}, \tag{30b}$$
$$A_m = \{e \in A(G) : \text{ the tail of } e \text{ is in } V_m\}, \tag{30c}$$
$$T_m = (\bar{V}_m, A_m) \text{ is a subgraph of } G. \tag{30d}$$

We first show that $V_1, V_2, \ldots, V_M$ and $V(C_1), \ldots, V(C_K)$ form a partition of the edge set of G, i.e.,

$$V(G) = \left(\bigcup_{k=1}^{K} V(C_k)\right) \bigcup \left(\bigcup_{m=1}^{M} V_m\right), \tag{31a}$$
$$V_m \cap V_c = \emptyset, \quad \forall m, s, . \tag{31b}$$
$$V_m \cap V(C_k) = \emptyset, \quad \forall m, k. \tag{31c}$$
$$V(C_k) \cap V(C_l) = \emptyset, \quad \forall k \neq l, \tag{31d}$$

For any vertex $v \notin \left(\bigcup_{k=1}^{K} V(C_k)\right)$, its first-touch-vertex w must be different from v (otherwise v would be in a certain cycle). Since w is in a cycle, denoted as C_{k_0}, there is a directed edge with head w; in addition, since w is a first-touch-vertex of $v \notin C_{k_0}$, then there must be another edge with head w. Thus the indegree of w is at least 2, which means $w \in R$. Thus $w = u_m$ for some m, which implies $v \in V_m$. Since any $v \notin \left(\bigcup_{k=1}^{K} V(C_k)\right)$ must belong to V_m for some m, we have proved (31a).

Since each vertex v has a unique first-touch-vertex, thus a vertex cannot lie in two different sets V_m and V_s, which proves (31b). Assume (31c) does not hold, i.e., there exists some $v \in V(C_k) \cap V_m$ for some k, m. Since the first-touch-vertex of v is v itself, according to (30a) we have $v = u_m$; but according to (30b) $v = u_m \notin V_m$, a contradiction. Thus (31c) holds. (31d) is obvious.

Next, we show that the edge sets of $T_1, \ldots, T_m$ and $C_1, \ldots, C_K$ form a partition of the edge set of G, i.e.,

$$A(G) = \left(\bigcup_{k=1}^{K} A(C_k)\right) \bigcup \left(\bigcup_{m=1}^{M} A(T_m)\right), \tag{32a}$$
$$A(T_m) \cap A(T_s) = \emptyset, \quad \forall m, s, . \tag{32b}$$
$$A(T_m) \cap A(C_k) = \emptyset, \quad \forall m, k. \tag{32c}$$
$$A(C_k) \cap A(C_l) = \emptyset, \quad \forall k \neq l, \tag{32d}$$

These relation can be proved easily by (31) and the definitions (30c) and (30d). For any edge $e_1 \in A(G) \backslash \left(\bigcup_{k=1}^{K} A(C_k)\right)$, we want to show that e_1 lies in at least one T_m. Suppose $e_1 = (v_0, v_1)$ where $v_0, v_1 \in V(G)$. Since e_1 is not in a cycle, $v_0 \notin V_c$, thus by (31a) we have $v_0 \in V_m$ for a certain m, which further implies $e_1 \in A_m = A(T_m)$ by the the definitions (30c) and (30d). Thus we proved (32a). Any edge e in $A(T_m)$ has a tail $u \in V(T_m)$, thus according to (31b) we know $u \notin V_s, \forall s \neq m$. By the definition (30c), we have $e \notin A_m = A(T_m)$, which proves (32b). Similarly, any edge e in $A(C_k)$ has a tail $u \in V(C_k)$, thus according to (31c) we know $u \notin V_m, \forall m$, thus we have $e \notin A_m = A(T_m)$, which proves (32c). The last one (32d) holds because the cycles are disjoint.

Finally, we prove that for any $m \in \{1, 2, \ldots, M\}$, T_m is a subtree of G with the root u_m. For any vertex v_0 in the subgraph T_m, consider the walk $W(v_0)$. Any path starting from v_0 must be part of $W(v_0)$. Starting from v_0 there is only one path from v_0 to u_m which is $W_1(v_0)$, according to Observation 2. Therefore, by the definition of directed tree, T_m is a directed tree with the root u_m.

E.5 Proof of Lemma 3

We utilize the result of Lemma 2 to prove Lemma 3. More specifically, we will reduce to the case of Lemma 2.

We build a new graph as follows. Denote the set of vertices in G that have outdegree 0 as D_0. For any vertice in D_0, we add an edge from D_0 to itself (a self-loop), and obtain a new graph $\tilde{G} = (V, \tilde{A})$. Now each vertice in $\tilde{G}$ has outdegree exactly 1.

Each self-loop is a length-1 cycle, thus by adding edges to vertices in D_0 we have created $|D_0|$ length-1 cycles, denoted as $C_{K+1}, \ldots, C_{K+|D_0|}$. Suppose all other cycles are $C_1, C_2, \ldots, C_K$.

According to Lemma 1, there exist cycles $C_1, C_2, \ldots, C_K, C_{K+1}, \ldots, C_{K+|D_0|}$ and subtrees $T_1, T_2, \ldots, T_M$ such that: (a) Each edge $v \in \tilde{A}$ appears either in exactly one of the cycles or in exactly one of the subtrees. (b) The root of each subtree u_m is a vertex of a certain cycle C_k where $1 \leq k \leq K + |D_0|$. In addition, each vertex of the graph appears in exactly one of the following sets: $V(C_1), \ldots, V(C_K), V(T_1)\backslash\{u_1\}, \ldots, V(T_M)\backslash\{u_M\}$,

Now we remove the edges added to vertices in D_0 and restore the original graph. Then we have removed the cycles $C_{K+1}, \ldots, C_{K+|D_0|}$ and do not change other cycles and subtrees. We do change the relations between the trees and the cycles: previously, the root of each tree is a vertex in a certain cycle; now, since some cycles are removed, the roots of some trees will be a vertex with outdegree 0. Suppose these trees are $T_{M_0+1}, T_{M_0+2}, \ldots, T_M$.

After removing the edges added to vertices in D_0, $C_1, C_2, \ldots, C_K$ and subtrees $T_1, T_2, \ldots, T_M$ satisfy the following: (a) Each edge $v \in A$ appears either in exactly one of the cycles or in exactly one of the subtrees. (b) Denote the root of subtree T_m as u_m, $m = 1, \ldots, M$. Then u_m is either a vertex of a certain cycle C_k where $1 \leq k \leq K$, or a vertex with outdegree 0. (c) Each vertex of the graph appears in exactly one of the following sets: $V(C_1), \ldots, V(C_K), V(T_1)\backslash\{u_1\}, \ldots, V(T_{M_0})\backslash\{u_{M_0}\}$, $V(T_{M_0+1}), \ldots, V(T_M)$.

E.6 Proof of Claim E.1

We first prove the case for $d \geq 2$. Suppose the corresponding graph for Y is G, and G is decomposed into the union of cycles $C_1, \ldots, C_K$ and trees $T_1, \ldots, T_m$. We perform the following operation: pick an arbitrary tree T_m with the root u_m. We claim that there must be an edge e with the head u_m. If $u_m > n$ (i.e. u_m represents some y_i), then there must be an incoming edge to u_m, thus the claim holds. If $u_m \leq n$ (i.e. u_m represents some x_i), then u_m must have an outgoing edge, and this edge must be in a cycle (otherwise u_m cannot be the root). Thus u_m is chosen to be in a tree T_m must because u_m is a head of an edge.

Suppose v is the tail of the edge e. Now we remove the edge $e = (v, u_m)$ and create a new edge $e' = (v, v)$. The new edge corresponds to $y_v = x_v$. The old edge (v, u_m) corresponds to $y_v = x_{u_m}$ (and a term $\xi(f(x_{u_m}) - f(x_v))$) if $u_m \leq n$ or $y_v = y_{u_m - n} \notin \{x_1, \ldots, x_n\}$ (and a term $\xi(f(y_{u_m-n}) - f(x_v))$) if $u_m > n$. This change corresponds to the change of y_v: we change $y_v = x_{u_m}$ (if $u_m \leq n$) or $y_v = y_{u_m-n}$ (if $u_m > n$) to $\hat{y}_v = x_v$. Let $\hat{y}_i = y_i$ for any $i \neq v$.

Previously v is in a tree T_m, now v is the head of a new tree, and also part of the new cycle $C_{K+1} = (v, e', v)$. In this new graph, the number of vertices in cycles increases by 1, thus the value of g increases by $-\frac{1}{n}\log 2$, i.e., $g(\hat{Y}) - g(Y) = \frac{1}{n}\log 2$.

Since $d \geq 2$, we can find a path in $\mathbb{R}^d$ from a point to another point without passing any of the points in $\{x_1, \ldots, x_n\}$. In the continuous process of moving y_v to $\hat{y}_v$, the function values will not change except at the end that $y_v = x_v$. Thus there is a non-increasing path from Y to $\hat{Y}$, in the sense that along this path the function values of g does not decrease.

The illustration of this proof is given as below.

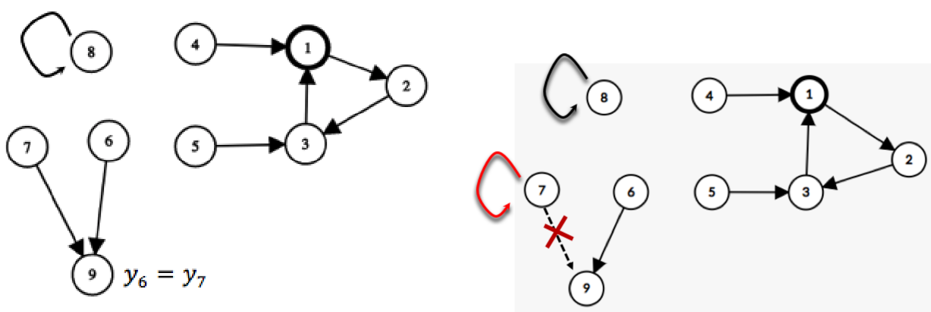

(a) Original graph

(b) Modified graph, with improved function value

Figure 6: Illustration of the proof of Claim E.1. For the figure on the left, we pick an arbitrary tree with the head being vertex 9, which corresponds to $y_6 = y_7$. We change y_7 to $\hat{y}_7 = x_7$ to obtain the figure on the right. Since one more cycle is created, the function value increases by $-\frac{1}{n}\log 2$.

For the case $d = 1$, the above proof does not work. The reason is that the path from y_v to $\hat{y}_v$ may touch other points in $\{x_1, \ldots, x_n\}$ and thus may change the value of g. We only need to make a small modification: we move y_v in $\mathbb{R}$ until it touches a certain x_i that corresponds to a vertex in the tree T_m, at which point a cycle is created, and the function value increases by at least $\frac{1}{n}\log 2$. This path is a non-decreasing path, thus the claim is also proved.